# SRF 2023 Tutorial: RF Coupler

June 2023

Sang-hoon Kim

Facility for Rare Isotope Beams, Michigan State University

# Contents

# Introduction

- This talk will cover RF power coupler, also known as fundamental power coupler (FPC), main coupler (MC), main power coupler (MPC), high power coupler, …
- For HOM damping using HOM couplers, please see the next lecture, “Cavity Beam Interaction/HOMs and Dampers” by Michiru Nishiwaki (KEK). We will briefly see testing and operation aspects when RF couplers are integrated with cavity, but no in detail. You may find more information about testing from the previous lecture, “Cavity Testing” by Walter Hartung (FRIB).
- Since my direct experience focuses on <~20 kW CW coaxial couplers, you may also find useful information for high power couplers (>~100 kW) from the previous SRF tutorials, particularly about fabrication and coupler conditioning aspects:
  - SRF 2021: E. Montesinos (CERN), “High Power Couplers and HOM Couplers”
  - SRF 2019: E. Kako (KEK), “High Power Couplers and HOM Couplers”
  - SRF 2017: E. Montesinos (CERN), “High Power Couplers and HOM Couplers”
  - SRF 2015: G. Devanz (CEA-Saclay), “Fundamental Power Couplers and HOM Couplers”
  - SRF 2013: E. Kako (KEK), “High Power Input Couplers and HOM Couplers for Superconducting Cavities”
  - SRF 2011: W.-D. Moeller (DESY), “Design and Fabrication Issues of High Power and HOM Couplers”

# What is a coupler for superconducting cryomodules?

**An example: two-window FPC for APS-U 1.4 GHz high harmonic cavity, CW 20 kW Traveling-wave [1]**

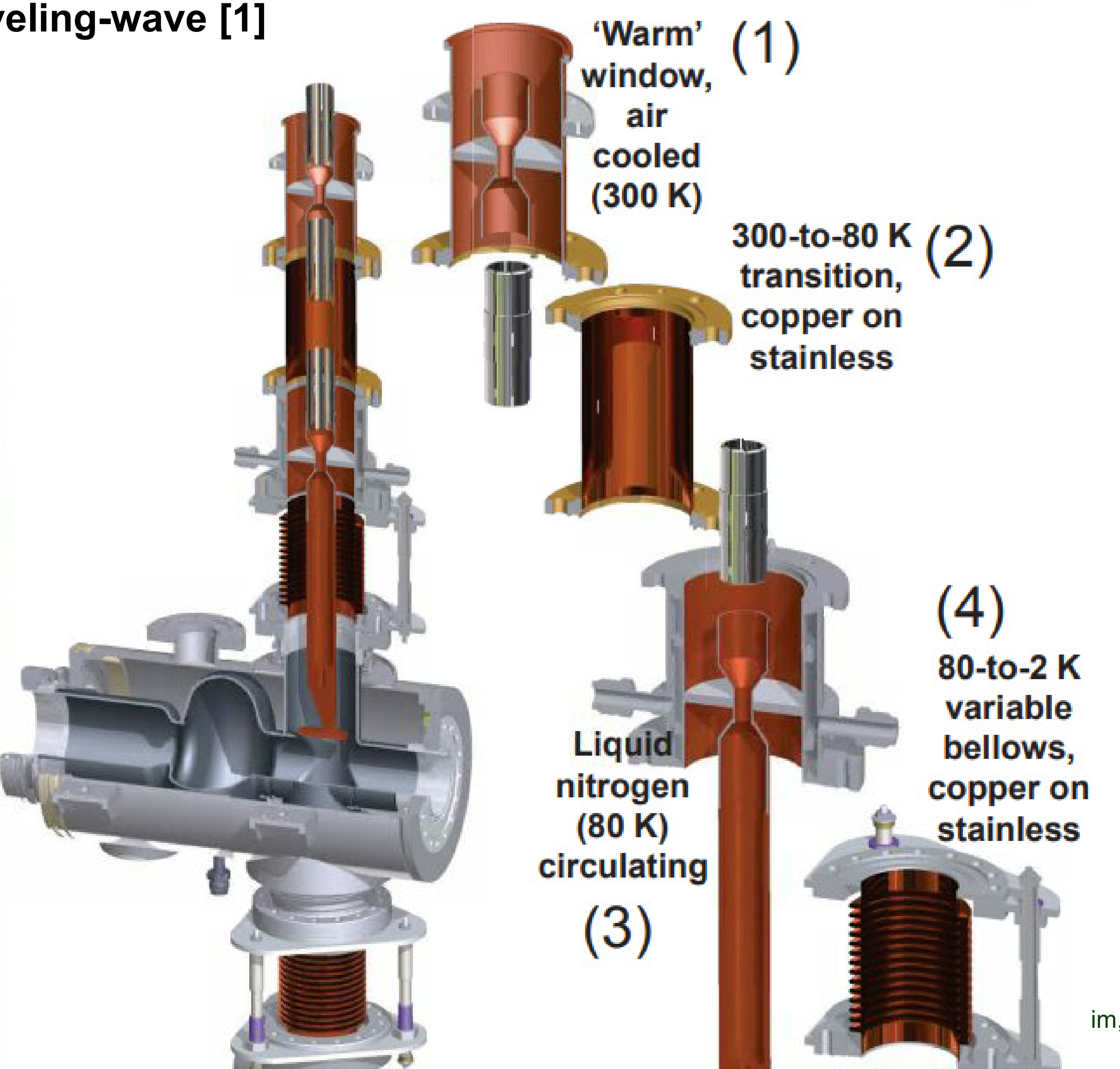


- **Impedance matched transmission line**
- **RF window(s) for vacuum break but RF transmission**
- **Antenna for design coupling strength**
- **Cooling RF loss on normal conducting walls**
- **Thermal transitions: RT -> shield, shield -> cavity to minimize conductive heat leaks**

# Various Couplers: Single Window Coax

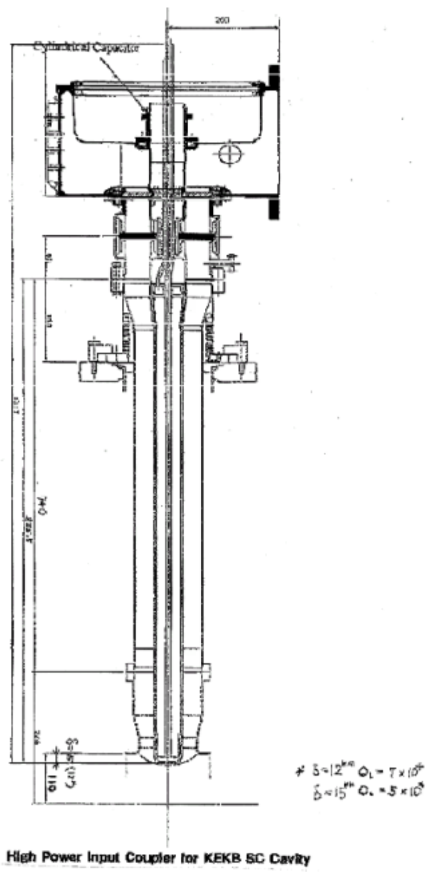


KEKB Input Coupler [2]

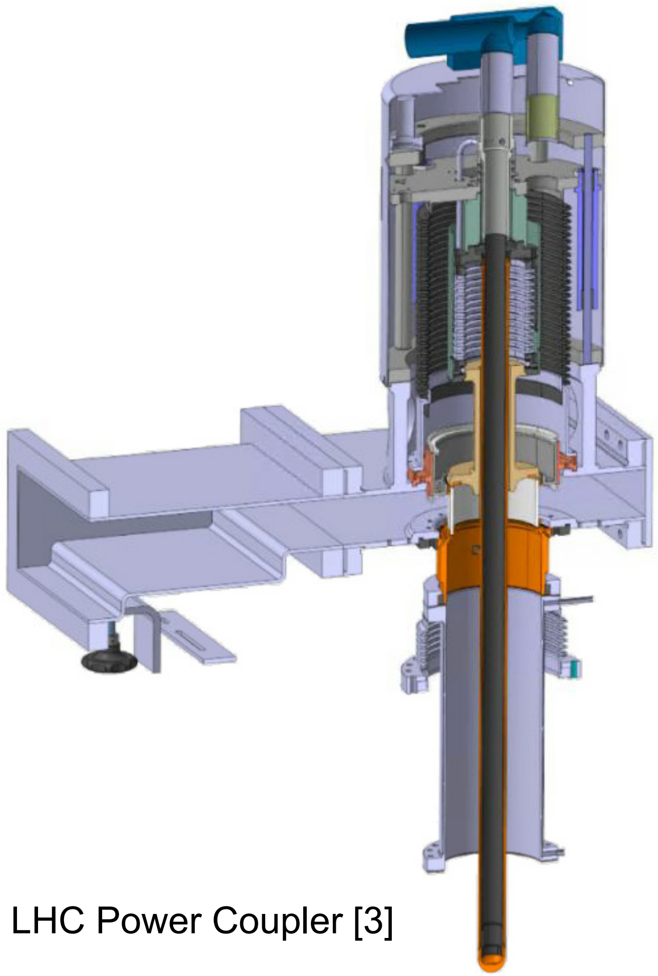

LHC Power Coupler [3]

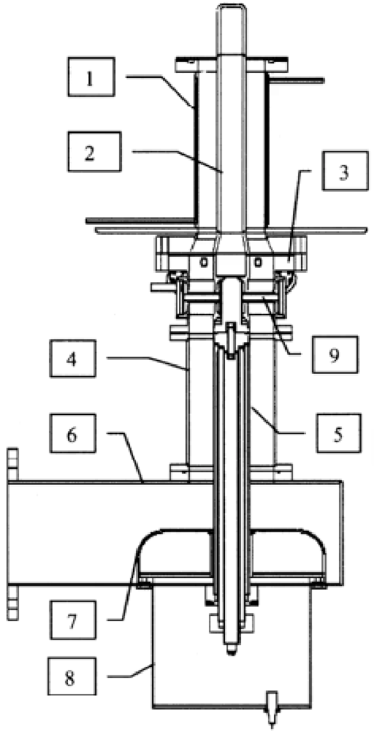


SNS FPC [4]


[2] Y. Kijima et al., “Input coupler of superconducting cavity for KEKB,” Proc. EPAC’00, p. 2040.
[3] E. Montesinos, “Power couplers and HOM dampers at CERN,” ERL17.
[4] I. E. Campisi et al., “the fundamental power coupler prototype for the spallation neutron source (SNS) superconducting cavities,” Proc. PAC2001, p. 1140.

# Various Couplers: Double Window Coax

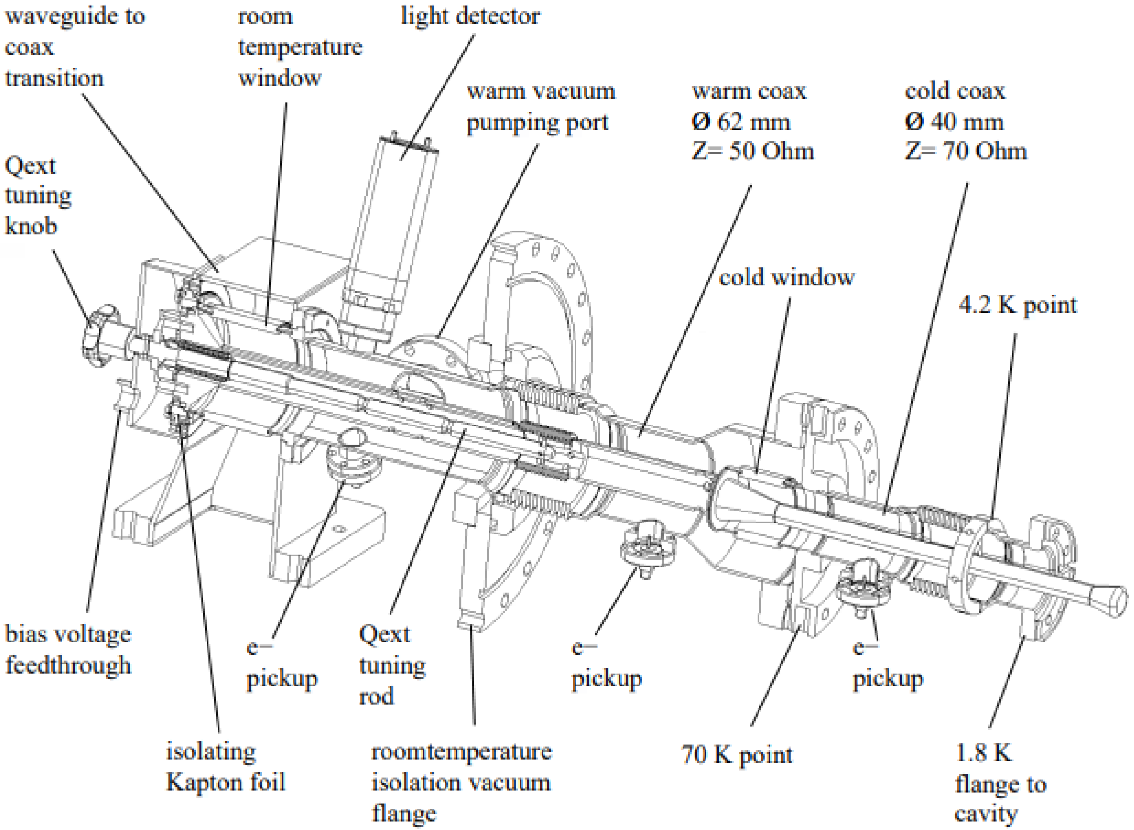


TTF-III Coupler [5]

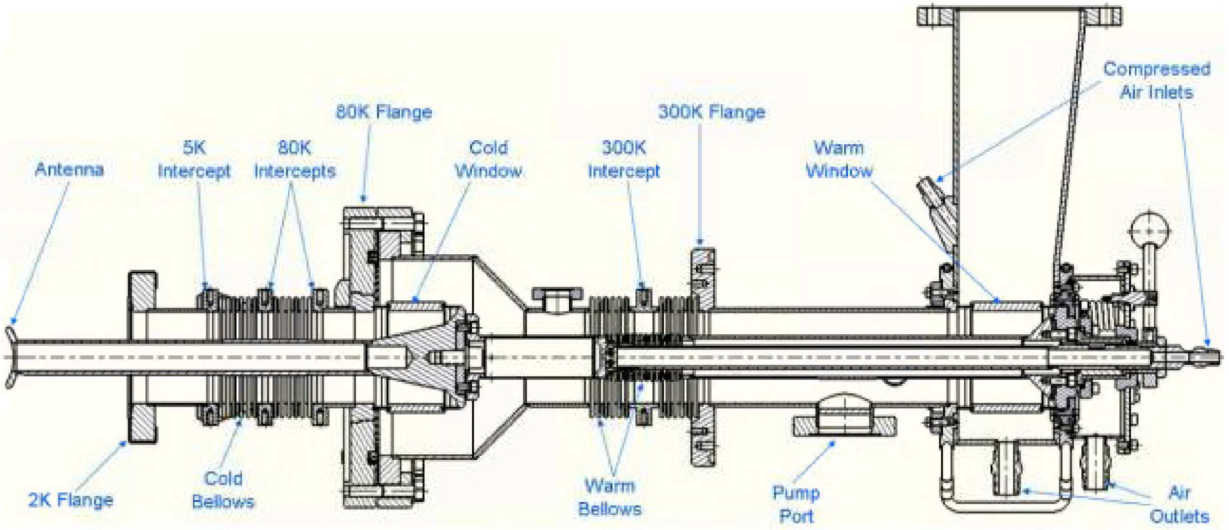


Cornell ERL Injector Coupler [6]


[5] W.D. Moeller, “High power coupler for the TESLA Test Facility,” Proc. SRF1999, p. 577.
[6] V. Veshcherevic et al., “High power tests of first input couplers for Cornell ERL injector cavities,” Proc. PAC07, p. 2355.

# Various Couplers: Waveguide

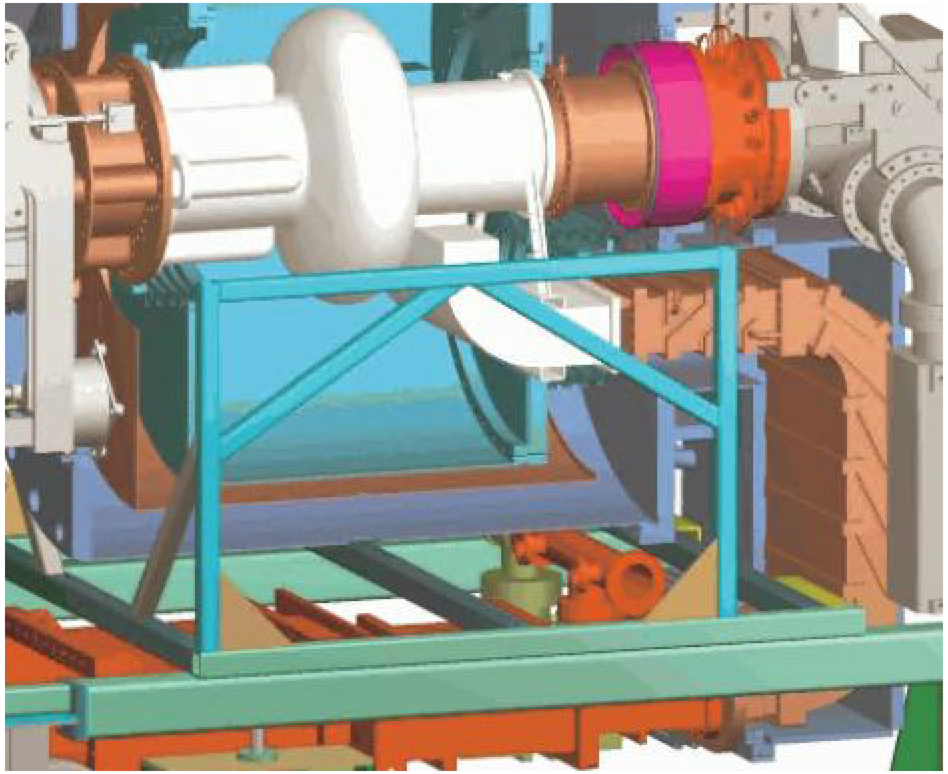

CESR IR module [7]

[7] S. Belomestnykh and H. Padamsee, “Performance of the CESR superconducting RF system and future plans,” Proc. SRF2001, p. 197.

# Waveguide, Single Window Couplers

WG, Fixed

- CESR-3 @ Cornell: 500 MHz, tested at 450 kW CW TW, Operated at 360 kW CW, Qext = 2e5

Coax, Fixed

- KEK-B @ KEK: 508 MHz, test: 800 kW CW TW, op: 380 kW CW, Qext = 7e4, disk
- SNS @ ORNL: 805 MHz, test: 2.0 MW pulsed, op: 350 kW pulsed, duty: 1.3 ms x 60 Hz, Qext = 7e5, disk
- SPIRAL-2 @ GANIL: 88 MHz, test: 10 kW CW, op: 10 kW CW, Qext = 5e5, disk

Coax, variable

- LHC @ CERN: 400 MHz, test: 500 kW CW TW, Op: 300 kW CW, Qext = 2e4 – 3.5e5, disk

Developing, Coax fixed

- EIC @ BNL: 591 MHz, spec: CW 1 MW (TW)/ 500 kW (SW), Qext = 2e4 – 3.5e5, disk

# Double Window Couplers

Coax, variable

- TTF3 @ DESY: 1.3 GHz, test: 1.0 MW, 1.3 ms, 10 Hz, op: 350 kW, 1.3 ms, 10 Hz, Qext = 1e6 – 2e7, cylinder
- STF2 @ KEK: 1.3 GHz, test: 1.5 MW, 1.5 ms, 5 Hz, op: 450 kW, 1.5 ms, 5 Hz, Qext = 2e6 – 4e6, disk
- Cornell ERL Injector @ Cornell: 1.3 GHz, test: 60 kW CW, op: 40 kW CW, Qext, cylinder
- APS-U @ ANL: 1.4 GHz, test: 20 kW CW (TW), Qext = 2e5 – 2e7, disk

# (Minimum) Requirements

- Meet the design goal of the coupling strength and, if needed, provide adjustability?
- Impedance matching in the coupler transmission line?
- Heat loads are minimized and acceptable: conductive heat leaks (static) + RF losses (dynamic)?
- No issues in fabrication such as ceramic brazing, copper plating?
- No multipacting or RF breakdown issues?
- Particulate-free when assembled with cavities?
- Thermally and mechanically stable with RF and beam?
- No unexpected HOMs excited due to couplers?
- No impact due to cavity field emission?
- Enough instrumentation and interlocks to prevent from failures of coupler/cavity/cryomodule?
- … Ok, good enough for 1.5 hour talk

# Backgrounds

- Waveguide, resonant cavity, lumped circuit model, RF coupling
- Material properties at cryogenic temperatures
- Multipacting, RF breakdown

# Waveguides

## Rectangular waveguide

1.3 GHz TE10 mode
in WR650

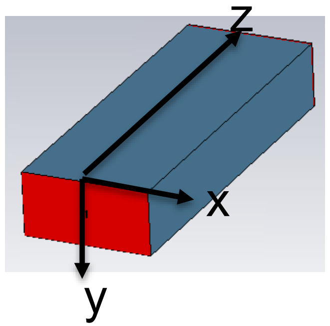


E-field on xy plane

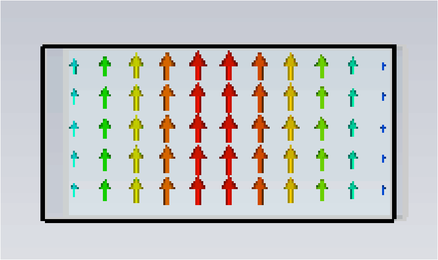

E-field on yz plane

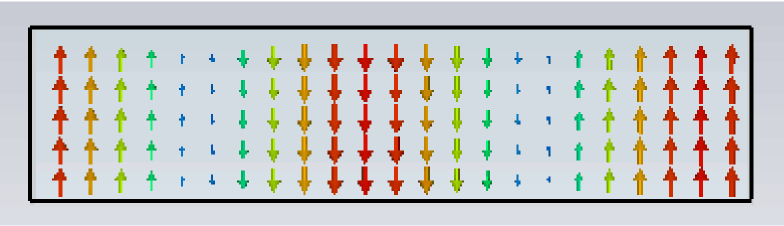

## Coaxial waveguide

1.3 GHz TEM mode
In 3-1/8” EIA Coax

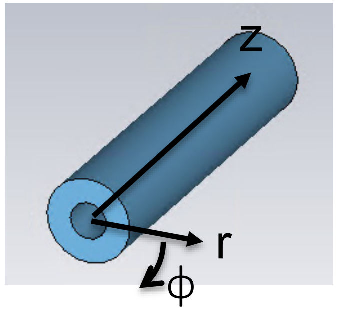


E-field on rϕ plane

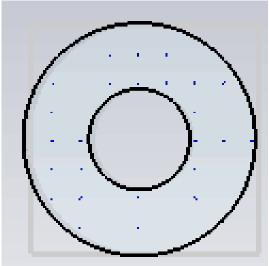

E-field on rz plane

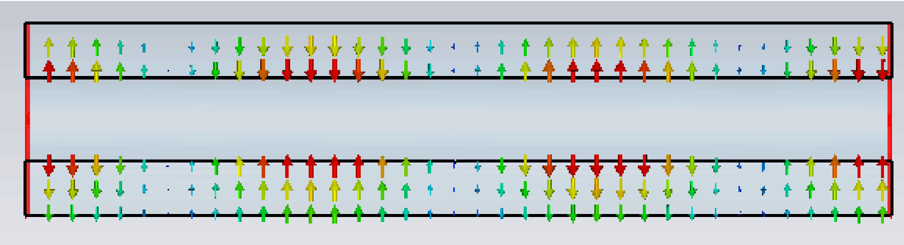

# Cutoff Frequency and Attenuation

- Cutoff frequency in a circular waveguide
  - $\text{TE}_{nm}$ mode: $f_{c,nm} = \frac{p'_{nm}}{2\pi a\sqrt{\epsilon\mu}}$, $\text{TM}_{nm}$ mode: $f_{c,nm} = \frac{p_{nm}}{2\pi a\sqrt{\epsilon\mu}}$, where $p'_{nm}$ and $p_{nm}$ are the m-th roots of $J'_n$ and $J_n$, respectively
- Wave with a frequency under the cutoff frequency is in the evanescent mode
  - Ex: 1.3 GHz TE11 and TM01 waves in 70 mm diameter circular waveguide

TE11

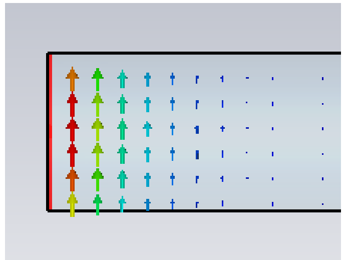

TM01

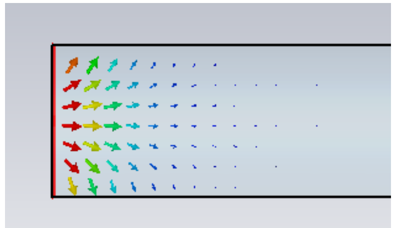

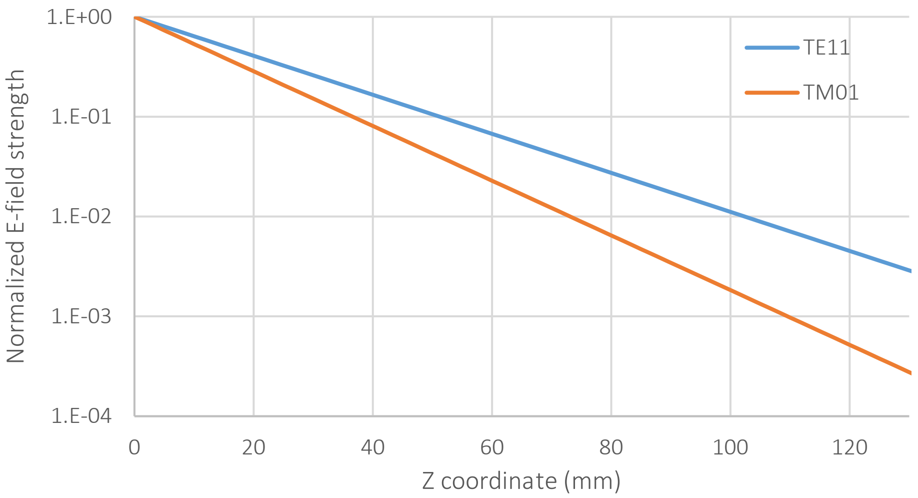


- In a coaxial waveguide, TEM mode does not have cutoff frequency while TE and TM modes have cutoff frequencies

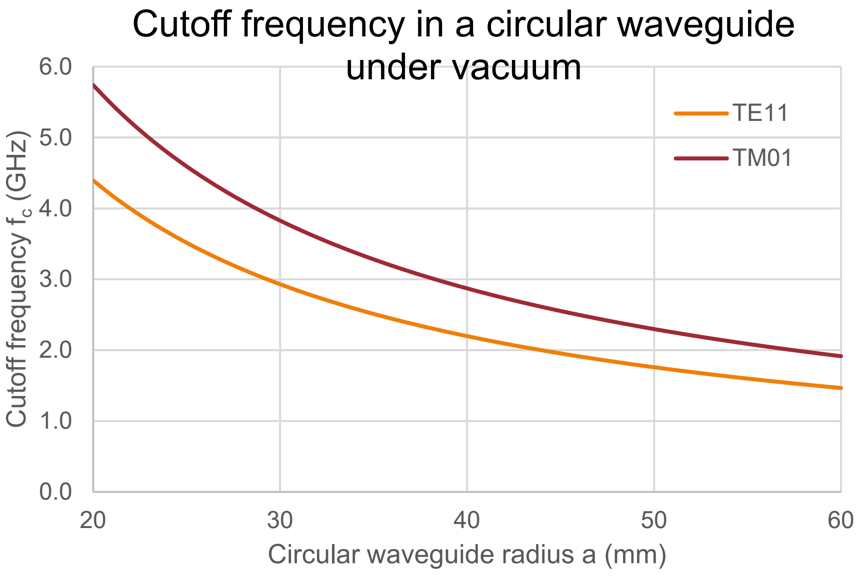


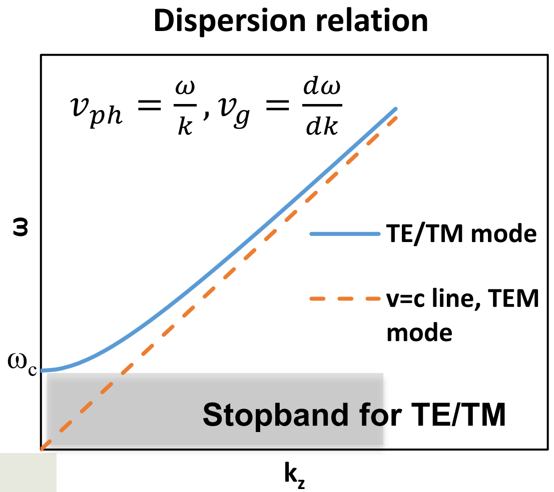

# Waveguide Coupling to Resonant Cavity

- Inductive coupling (by magnetic field)

**A rectangular WG coupled to 1-cell elliptical cavity via racetrack coupling slot**

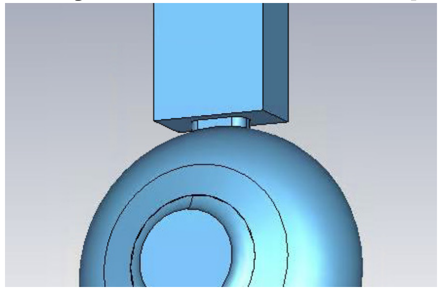

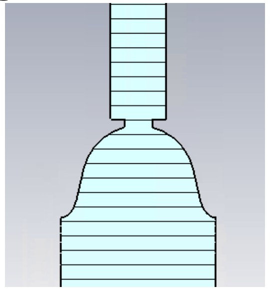

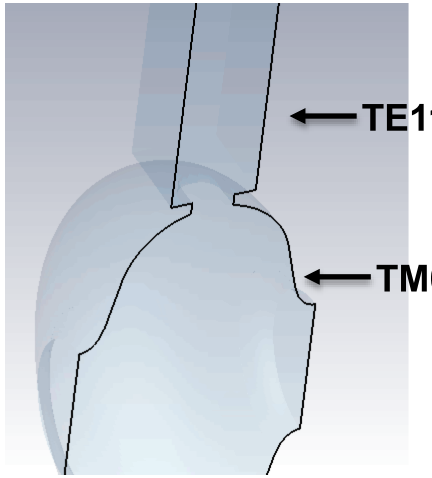

**TE11 in Rectangular WG**

**TM010 in cavity**

**For stronger coupling,**

**Place in a high B-field region and/or Increase inductance**

- Capacitive coupling (by electric field)

**FRIB HWR53 with FPC**

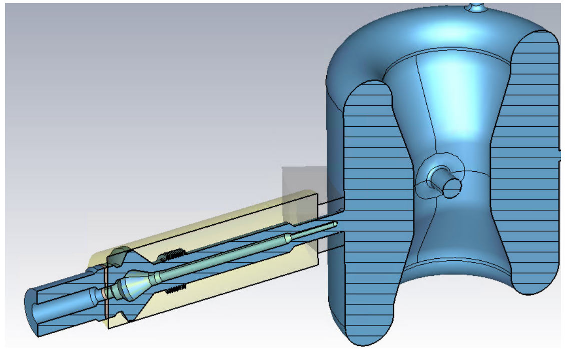

**TM01-like mode in the “transition” between cavity and coupler**

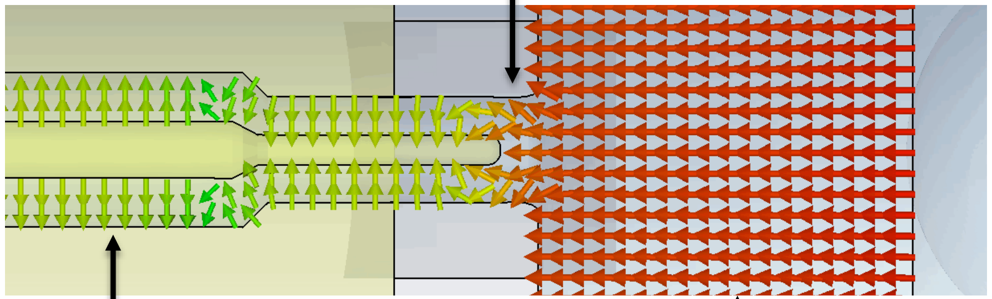

**TEM mode in FPC**

**HWR mode in cavity**

**Place in a high E-field region and/or increase capacitance**

# Lumped-Element Circuit Model and Parameters [8]

**RF system waveguide coupled to a resonant cavity**

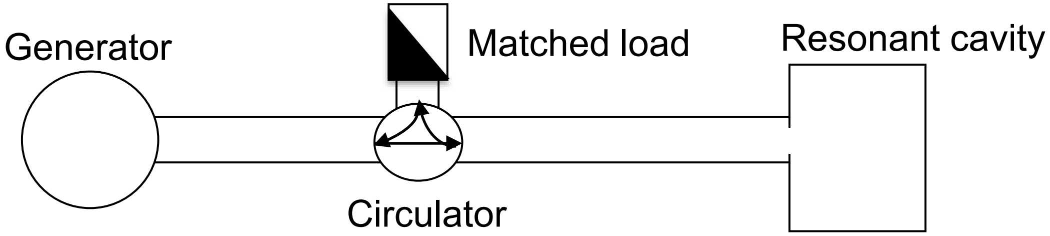


**Lumped circuit model**

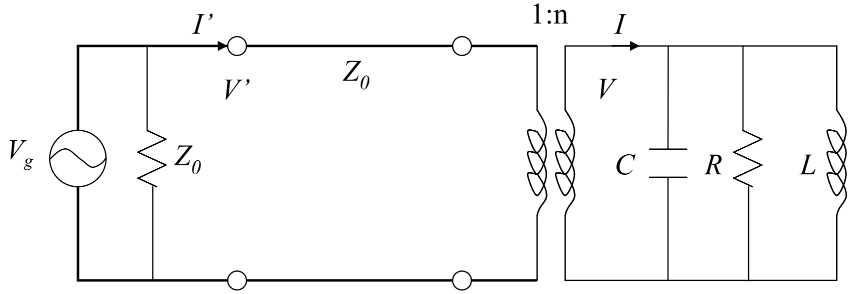


Cavity impedance

$$Z_c = \frac{1}{i\omega C + 1/i\omega L + 1/R}$$

**Simplified lumped circuit model**

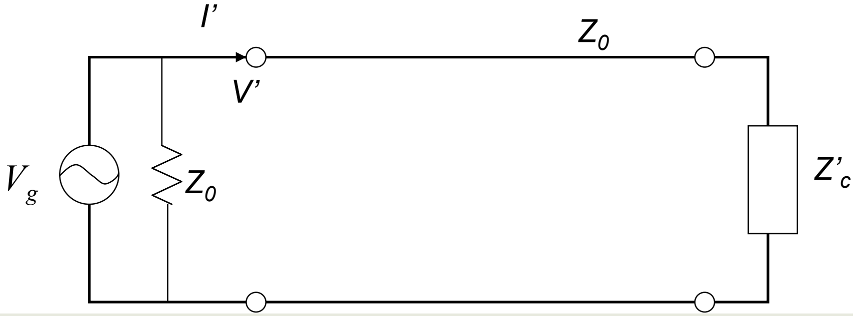


Equivalent cavity impedance in the primary circuit

$$Z_c' = \frac{I'}{V'} = \frac{1}{n^2}\frac{I}{V} = \frac{Z_c}{n^2}$$

- Quality factors
  - Unloaded Q: $Q_0 = \frac{\omega_0 U}{P_W} = \omega_0 RC$, $P_w$: cavity wall loss
  - **External Q**: $Q_{ext} = \frac{\omega_0 U}{P_{ext}} = \omega_0 n^2 Z_0 C$, $P_{ext}$: “external” power
  - Loaded Q: $\frac{1}{Q_L} = \frac{1}{Q_0} + \frac{1}{Q_{ext}}$
- **Coupling factor β**
  - $\beta \equiv P_{ext}/P_W = Q_0/Q_{ext} = R/n^2C$
    - » $\beta = 1$: critically coupled
    - » $\beta < 1$: undercoupled
    - » $\beta > 1$: overcoupled
- Relationship between β and reflection coefficient Γ
  - i) undercoupled case ($\beta < 1$):

$$|\Gamma| = \frac{1-\beta}{1+\beta}$$

  - ii) overcoupled case ($\beta > 1$):

$$|\Gamma| = \frac{\beta - 1}{\beta + 1}$$

*Note that the shunt impedance R here is in ‘circuit’ definition, which is ½ of the linac definition.

[8] T. Wangler, “RF Linear Accelerators,” (Wiley-VCH, Weinheim, 2008), pp. 135-148.

# RF Power Requirements without Beam, Transient Behavior of Reflected RF Power [8]

- $P_w = P_{fwd}(1 - |\Gamma|^2)$ and $P_w = \frac{\omega_0 U}{Q_0}$
  energy conservation: pickup Pext is negligible
- In a typical cryomodule case: $Q_{ext} \ll Q_0$ $(\beta \gg 1)$,

$$P_w = P_{fwd}(1 - |\Gamma|^2) = P_{fwd}\frac{4\beta}{(1+\beta)^2}$$

$$P_{fwd} = \frac{(1+\beta)^2}{4\beta}P_w, \quad P_w = \frac{\omega_0 U}{\beta Q_{ext}}$$

$$\therefore P_{fwd} \cong \frac{\omega_0 U}{4Q_{ext}} = \frac{1}{4Q_{ext}}\frac{V_{acc}^2}{r_s/Q}$$

when input RF is on resonant with cavity, i.e. $f_{RF} = f_0$

- Define a detuning angle $\psi$

$$\tan\psi = -2Q_L\delta, \ \delta \equiv (\omega - \omega_0)/\omega_0$$

$\omega$: drive rf frequency (also beam), $\omega_0$: cavity resonance

- Cavity impedance: $Z_L = \frac{Re^{i\psi}}{1+\beta}\cos\psi$,
  thus required FWD power with detuning:

$$P_{fwd}(\psi) = \frac{P_{fwd}(\psi = 0)}{\cos^2\psi}$$

  - If Δf = BW/2, $\psi = 45°$, $P_{fwd}(\psi = 45°) = 2P_{fwd}(\psi = 0)$, thus it will require twice higher power than resonance

*R is impedance in 'circuit' definition, equivalent to $r_s/2$, $r_s$ is the shunt impedance in 'linac' definition.

- The cavity field builds up with a time constant $\tau = 2Q_L/\omega_0$. Reflected voltage:

$$V_- = V_+\left[\underbrace{\frac{2\beta}{1+\beta}\left(1 - e^{-t/\tau}\right)}_{\text{Wave radiated from cavity}} \underbrace{- 1}_{\text{Wave nearly directly reflected from waveguide-to-cavity interface}}\right]$$

- In a typical cryomodule, reflected power $P_{ref}$ at RF off has ~4 times higher peak than $P_{fwd}$

Transient behaviors of reflected RF power

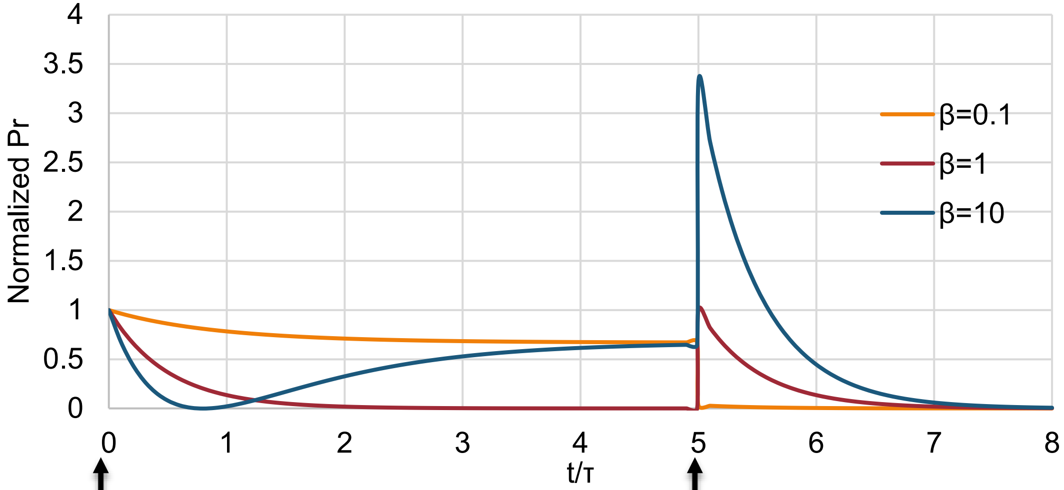


**RF on** **RF off**

[8] T. Wangler, "RF Linear Accelerators," (Wiley-VCH, Weinheim, 2008), pp. 135-148.

# RF Power Requirements with Beam [9]

- Phase notation
  - $V(t) = V_0 e^{i(\omega t+\phi)}$ $\longrightarrow$ $\tilde{V} = V_0 e^{i\phi}$, reference of $\phi$ is the crest of the wave, i.e. $\phi$=0 at the crest

    introduce a complex parameter eliminating time harmonics
- Beam loading effect
  - Beam-induced voltage $\tilde{V}_b = V_b e^{i(\pi+\psi)} = \frac{i_b r_s \cos\psi}{2(1+\beta)} e^{i(\pi+\psi)}$
  - Generator-induced voltage $\tilde{V}_g = V_g e^{i(\theta+\psi)} = \frac{2\sqrt{\beta r_s P_g}\cos\psi}{1+\beta} e^{i(\theta+\psi)}$
  - $\tilde{V}_c = \tilde{V}_b + \tilde{V}_g$
  - $i_b$: beam current, $r_s$: shunt impedance (linac definition),
  - $\beta$: coupling factor, determined/adjusted by **coupler (coupling strength)**
  - $\psi$: detuning angle, controlled by **frequency tuner**
  - $\theta$: phase of input RF, controlled by **RF control**
  - $P_g$: generator power, controlled by **RF control**

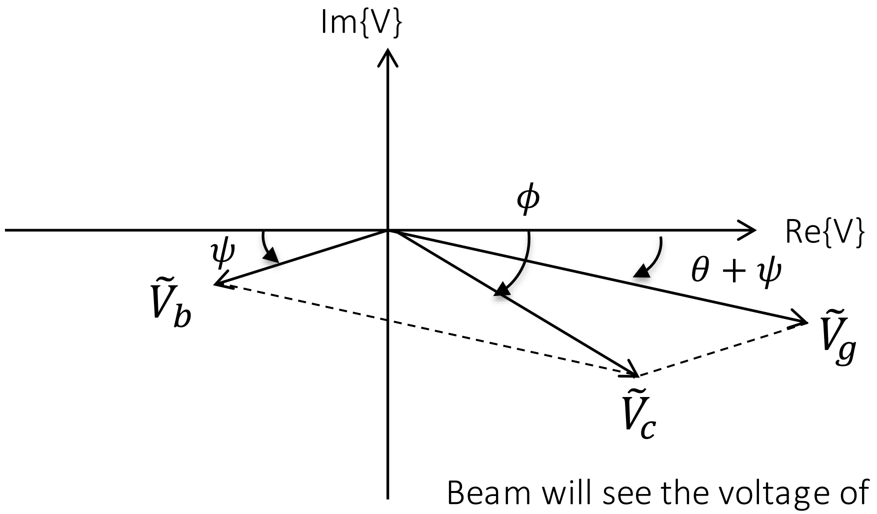


Beam will see the voltage of Vc at the phase $\phi$ referenced to the crest

[9] T. Wangler, "RF Linear Accelerators," (Wiley-VCH, Weinheim, 2008), pp. 347-351.

# Useful Relationships between External Q's and Scattering Parameters

- Recall the relationship between the reflection coefficient and coupling factor
  - If $\beta < 1, |\Gamma| = \frac{1-\beta}{1+\beta}$. Otherwise, $|\Gamma| = \frac{\beta-1}{\beta+1}$
- In a two-ports system, the transmission coefficient |T|, a.k.a. S21 in linear scale, can be represented by

$$|T| = S21 = \frac{2\sqrt{\beta_1\beta_2}}{(1+\beta_1+\beta_2)}$$

where $\beta_1 = Q_0/Q_{ext1}$, $\beta_2 = Q_0/Q_{ext2}$.

- Some examples:
  - In a cryomodule where FPC $Q_{ext1} \ll Q_0$, pickup $Q_{ext2} \gg Q_0$, i.e. $\beta_1 \gg 1, \beta_2 \ll 1$.

$$S21 \cong \frac{2\sqrt{\beta_1\beta_2}}{\beta_1} = 2\sqrt{\beta_2/\beta_1} = 2\sqrt{Q_{ext1}/Q_{ext2}} \longleftarrow$$

Almost independent of Q0

  - In a cavity with dual FPCs where $Q_{ext1} = Q_{ext2} \ll Q_0$, i.e. $\beta_1 = \beta_2 \gg 1$,

$$S21 \cong \frac{2\sqrt{\beta_1\beta_1}}{2\beta_1} = 1 \longleftarrow$$

Nearly traveling wave if RF is driven from one of the FPCs

: an example: coupler conditioning boxes in which two identical couplers are strongly coupled to a resonator box

# Dielectric Loss in RF Windows

- Dielectric loss in RF window

$$P_{loss} = \frac{\omega}{2}\int_V \epsilon'' \left|\vec{E}\right|^2 dv$$

- $\epsilon''$ : imaginary permittivity. The electrical loss tangent is introduced, defined by $\tan\delta = \epsilon''/\epsilon'$, $\epsilon'$: real permittivity

**Loss tangent of commercial polycrystalline alumina [10]**

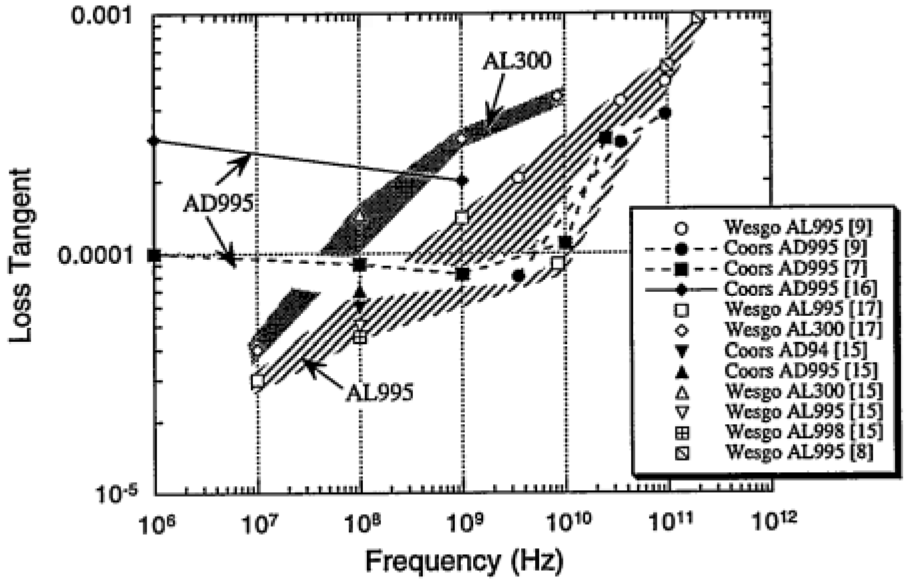


Fig. 2. Room temperature loss tangent vs. frequency for Wesgo AL300, AL995, AL998 [8,9,15,17] and Coors AD94, AD995 [7,9,15,16] grades of polycrystalline alumina.

Purity
AL995: 99.3 – 99.5%
AL300: 97.3%
AD995: 99.5%
AD94: 93.4%


[10] Zinkle, S.J., & Goulding, R.H. (1996). Loss tangent measurements on unirradiated alumina (DOE/ER--0313/19). United States.

# Wall Dissipation Powers on Coupler Walls

- Wall dissipation power due to normal skin effect

$$P_W = \frac{R_s}{2}\int_S \left|\vec{H}\right|^2 da\,,$$

where $R_s = \sqrt{\frac{\omega\mu}{2\sigma}} = \frac{1}{\sigma\delta_s}$, $\sigma$: electrical conductivity and $\delta_s$: normal skin depth

- Electrical resistivity ($\rho = 1/\sigma$) of copper and stainless steel at cryogenic temperatures*

Copper [11]

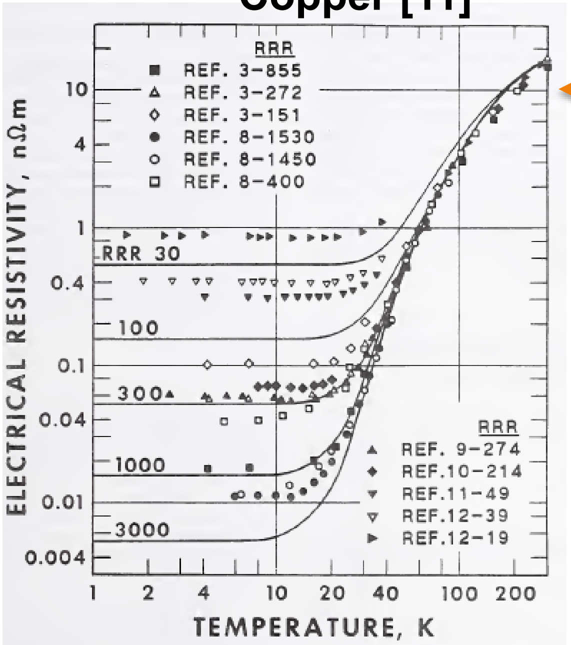


1e-8 Ohm*m

304 Stainless steel [12]

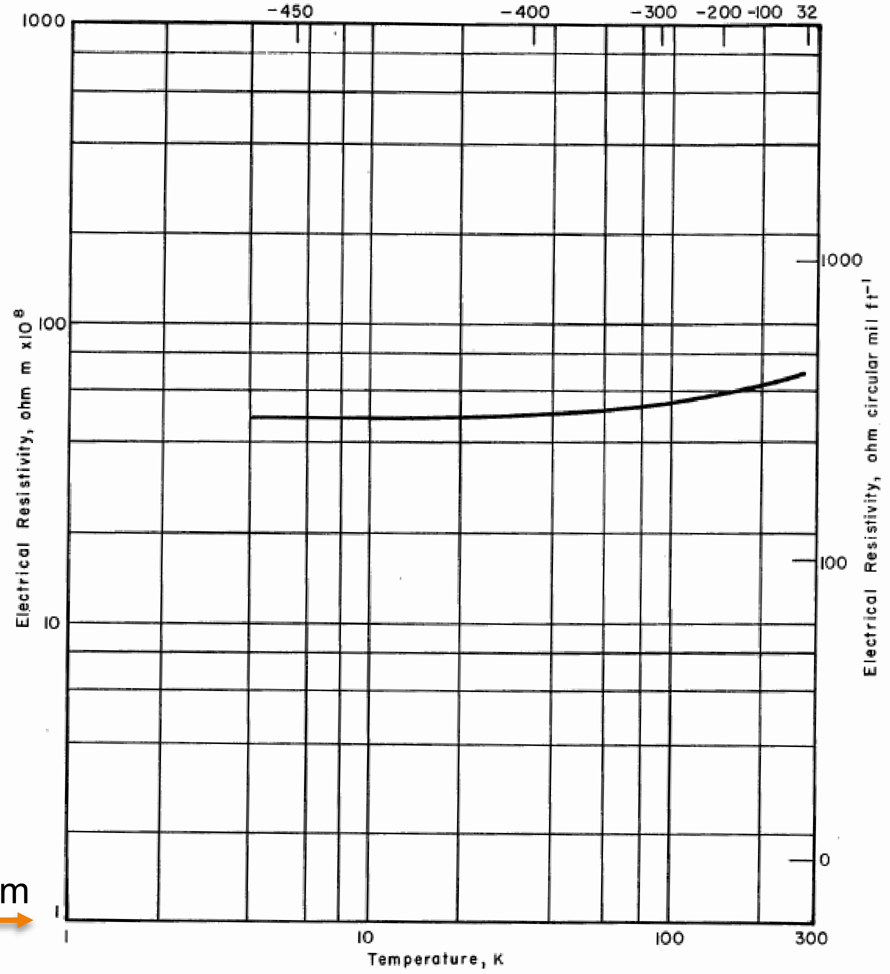


1e-8 Ohm*m

ELECTRICAL RESISTIVITY VERSUS TEMPERATURE FOR TYPE 304L STAINLESS STEEL

Need to use **copper surfaces** in high-power RF couplers to minimize wall dissipation powers


[11] N.J. Simon et al., "Properties of copper and copper alloys at cryogenic temperatures," NIST Monograph 117 (1992).
[12] J.E. Jensen, Brookhaven National Laboratory Selected Cryogenic Data Handbook (1980)

# Anomalous Skin Effect

- The normal skin effect is not valid anymore if electron mean free path $l$ is much larger than the skin depth $\delta$ $(l \gg \delta)$ [13]

$$l = \frac{\sigma m V_f}{n e^2}$$

$\sigma$: conductivity, $V_f$: Fermi speed, $n$: free electron density

- In this anomalous regime, effective number of electrons that contribute to conduction is of order of $n_{eff} = (\delta_a / l) n$, thus effective conductivity $\sigma_{eff} = (\delta_a / l) \sigma$.
- Anomalous skin depth is saturated earlier than expected from nomal skin depth, particular for high RRR and high frequency.
- Practically a couple of tens RRR would be good enough for 1.3 GHz [14]

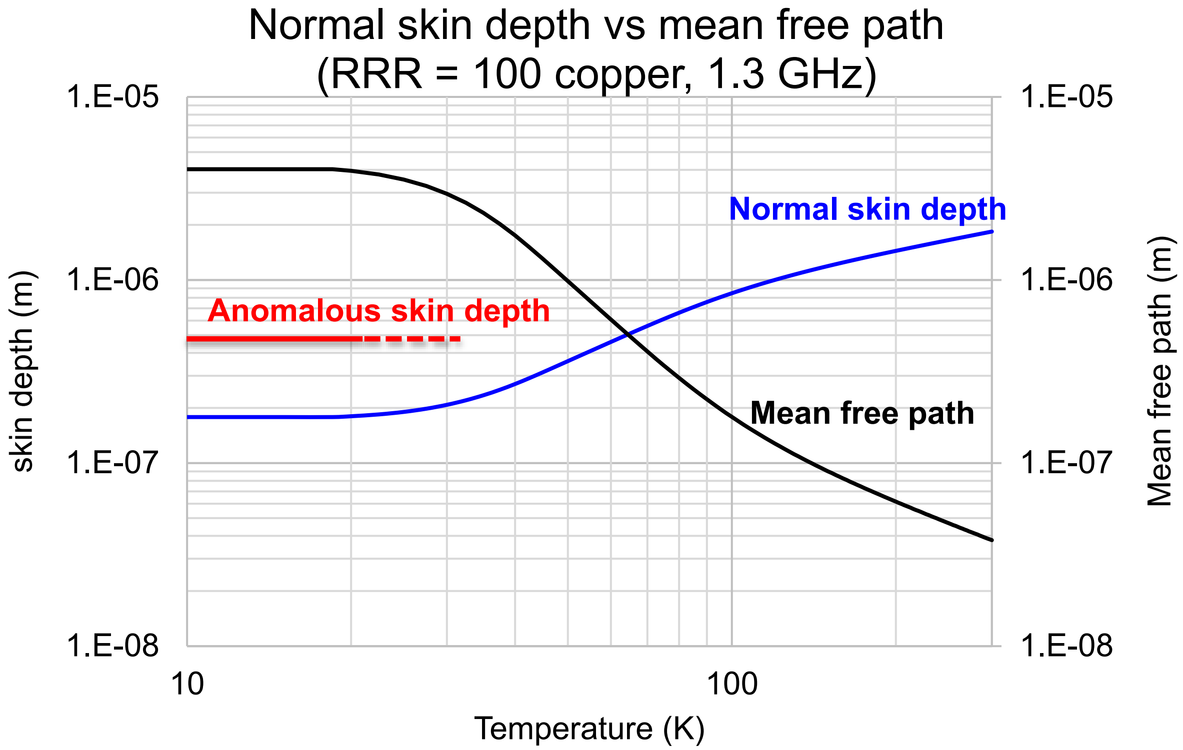



[13] R.G. Chambers, “The Anomalous Skin Effect,” Proceedings of the Royal Society of London. Series A, Mathematical and Physical Sciences, Vol. 215, No. 1123 (Dec. 22, 1952), pp. 481-497.
[14] W. Signer, D. Dwersteg, “Influence of heat treatment on thin electrodeposited cu layer,” Proc SRF’95, p. 653 (1995).

# Thermal Conductivity at Cryogenic Temperatures

**Copper [15]**

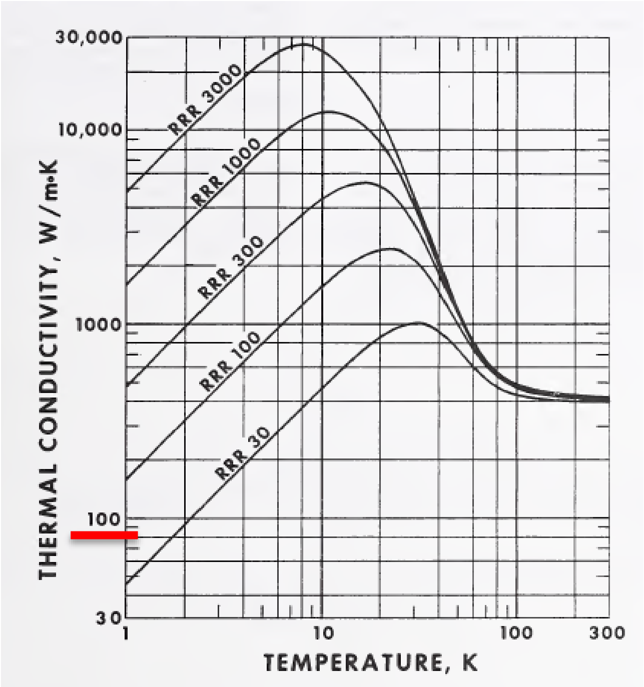


**304 stainless steel [16]**

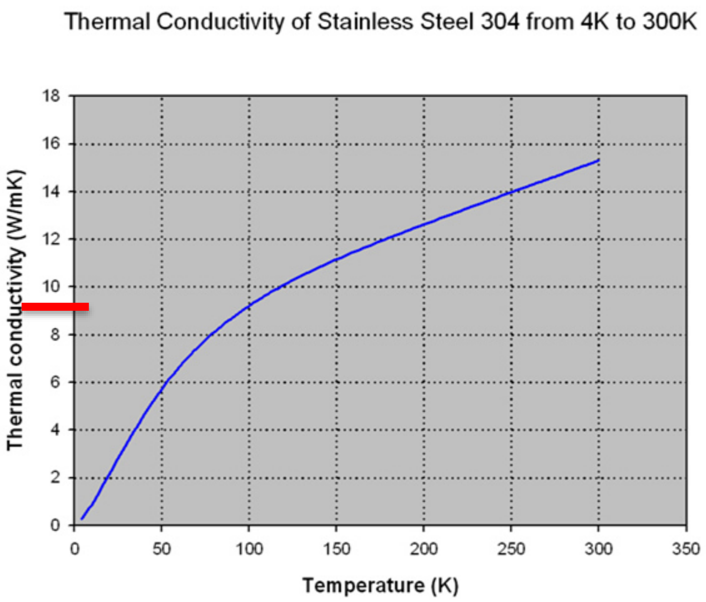


**Alumina**

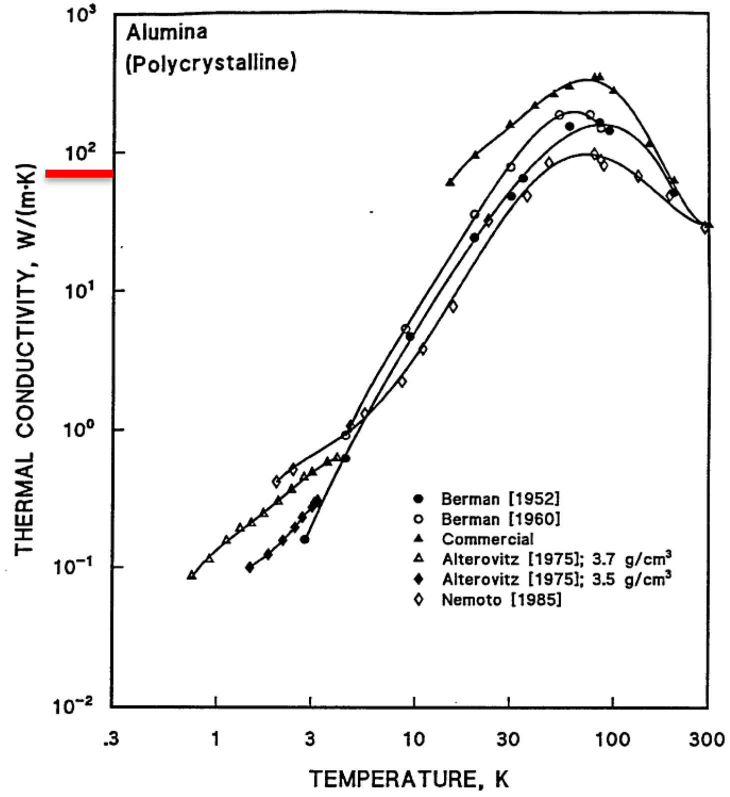


**Stainless steel wall** is superior to minimize **conductive heat leaks** while **copper surfaces** are needed to minimize **wall dissipation power (dynamic heat loads)**:
Thus FPCs use **copper-plated stainless steel**

*Alumina is a good thermal conductor at thermal shield temperatures*


[15] J.G. Hust, A.B. Lankford, "Thermal conductivity of aluminum, copper, iron, and tungsten for temperatures from 1K to the melting point," NBSIR 84-3007 (1984)
[16] NIST Cryogenic Material Properties


$Al_2O_3$ vs. temperature.
.tz et al. [1975],
.tions therein].

47

# Multipacting in Waveguides

- MP happens when "both" conditions are met:
  - **Resonance**: Electron time-of-flight is equivalent to integer times half of the RF period **AND**
  - **Amplification**: When electrons hit the surfaces with energies gained by RF E-field, secondary electron yield (SEY) at the electron impact energy is higher than one

**2-point MP**

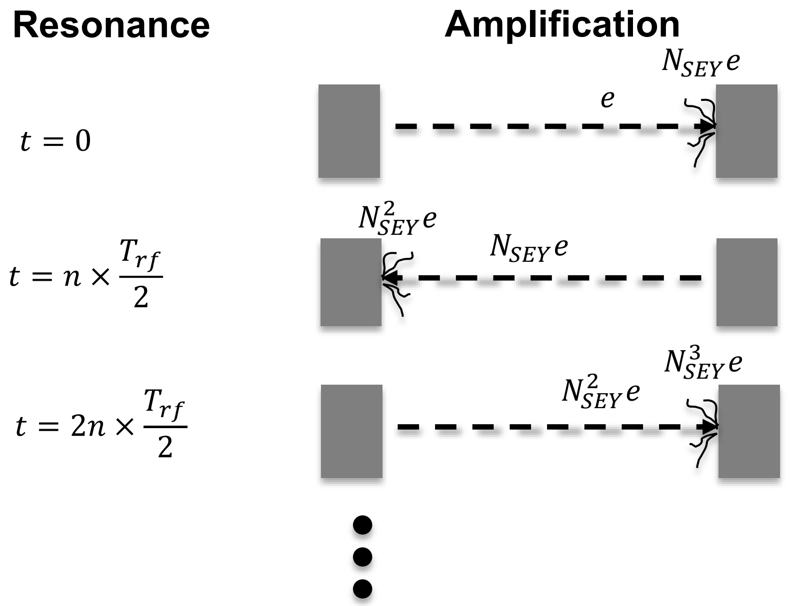


**Multipacting bands in coaxial waveguides [17]**

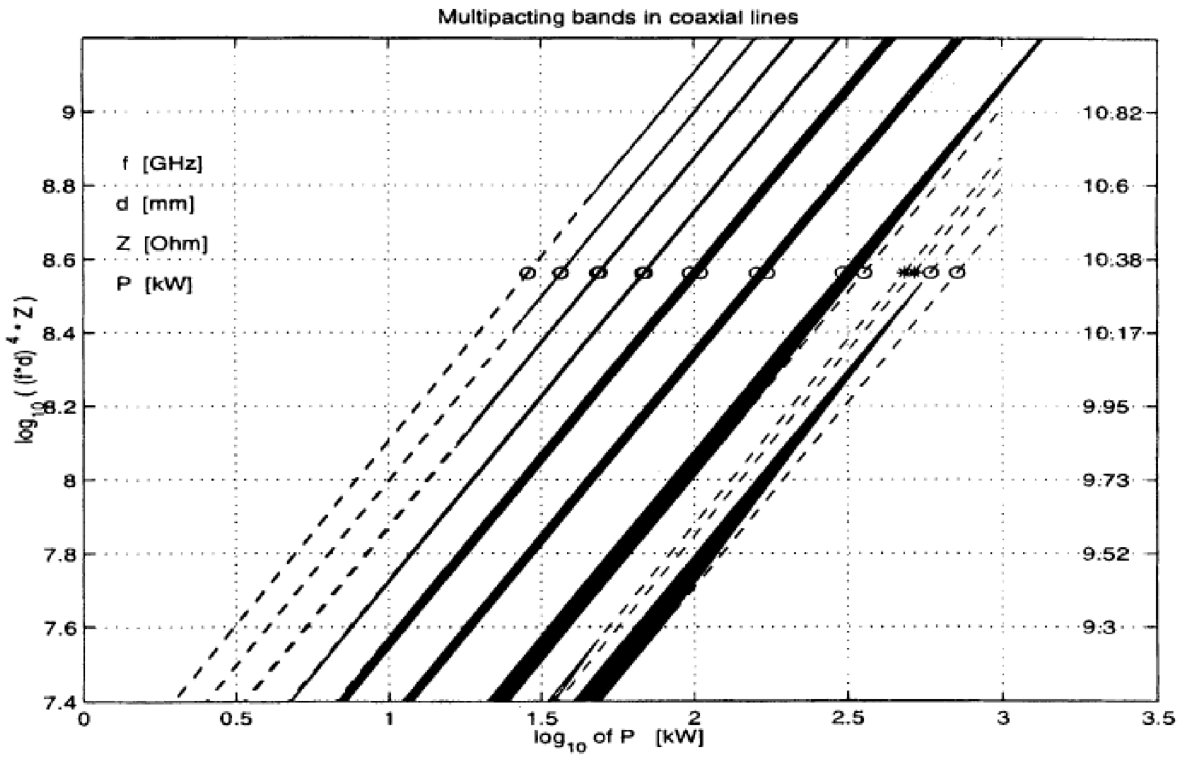


[17] E. Somersalo et al., "COMPUTATIONAL METHODS FOR ANALYZING ELECTRON MULTIPACTING IN RF STRUCTURES," Particle Accelerators, Vol. 59, pp. 107-141.

# RF Breakdown

- Kilpatrick criteria
  - Usually not relevant in SRF cavities, particular at low frequencies
  - FPC E-fields are usually well below these thresholds

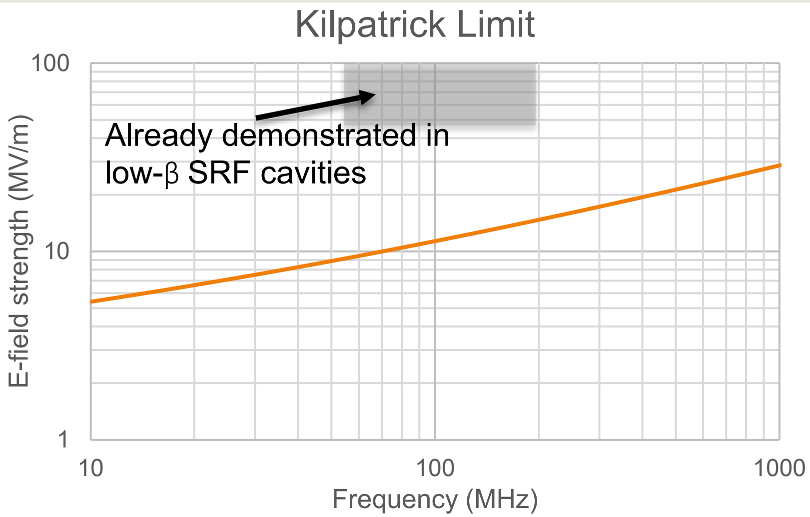


- Microwave breakdown
  - This can happen if the local vacuum on coupler surfaces increases due to, e.g., multipacting

**An example of microwave Paschen's curve [18]**

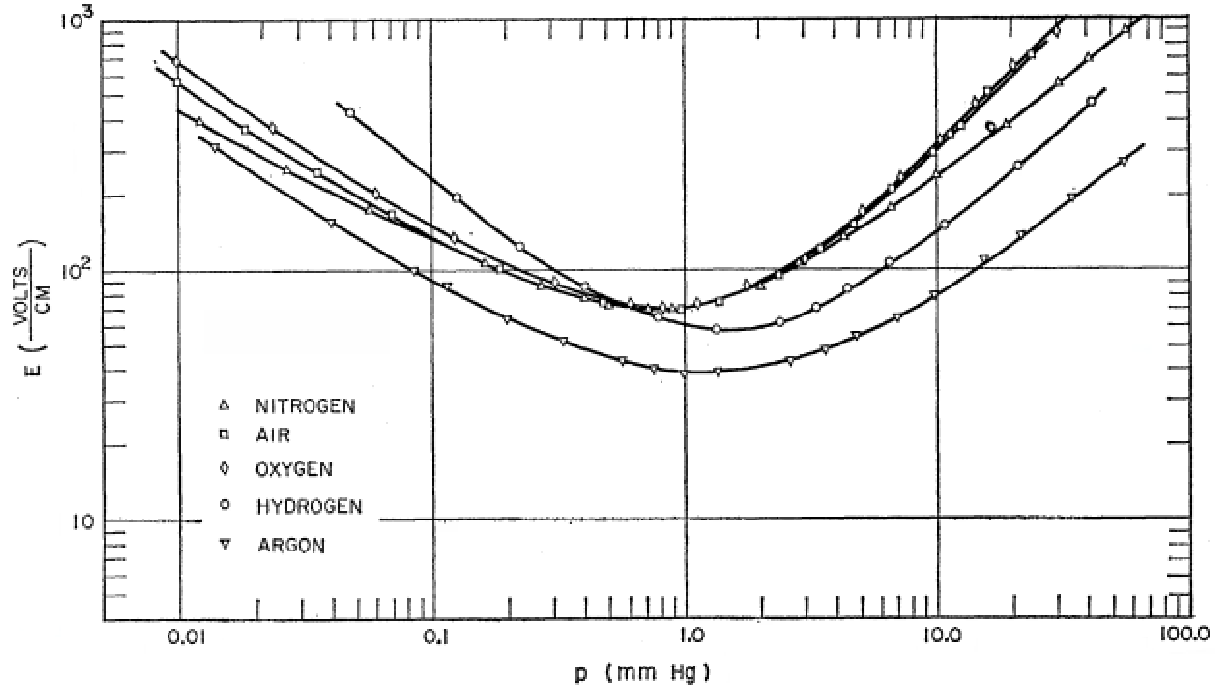


FIG. 2. Cw breakdown fields in nitrogen, oxygen, air, hydrogen, and argon at a frequency of 994 Mc/sec. (Characteristic diffusion length $\Lambda = 1.51$ cm.)

**Depends on frequency and system length scale**

[18] A.D. Macdonalds, et al., "Microwave Breakdown in Air, Oxygen, and Nitrogen," Phys. Rev. **130**, 1841 (1963).

# Design Considerations and Simulation Techniques

- Coupling strength, impedance matching
- Static and dynamic heat loads
- Multipacting and field emission
- HOMs: HOM coupler, coupler-induced HOM and extraction

# $Q_{ext}$ Calculation
# In Case of CST Microwave Studio (MWS)

**Example: LCLS-II-HE SRFgun cavity integrated with the FPC**

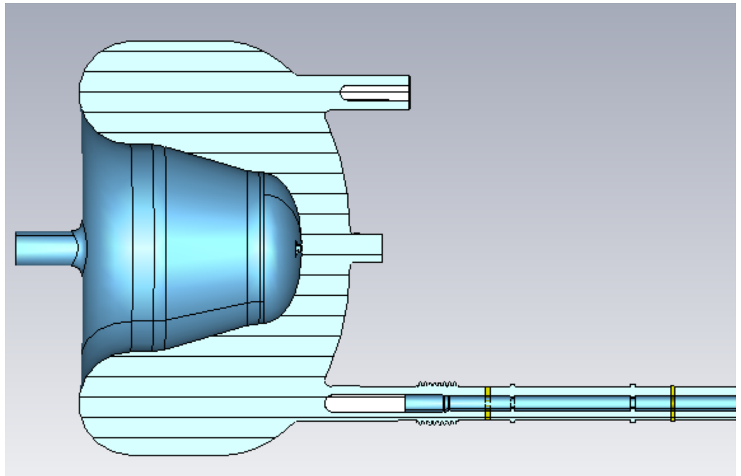

- Eigenmode Solver
  - Calculate Qext from postprocessing of two separate simulations with different boundary conditions at the waveguide port [100]

$Q_{ext}$ = 6.1e6

- Frequency-domain Solver
  - Sweep frequency and find a bandwidth of S21
  - Since background material is PEC, $Q_{ext} = Q_L$, pickup $Q_{ext2}$ is negligible

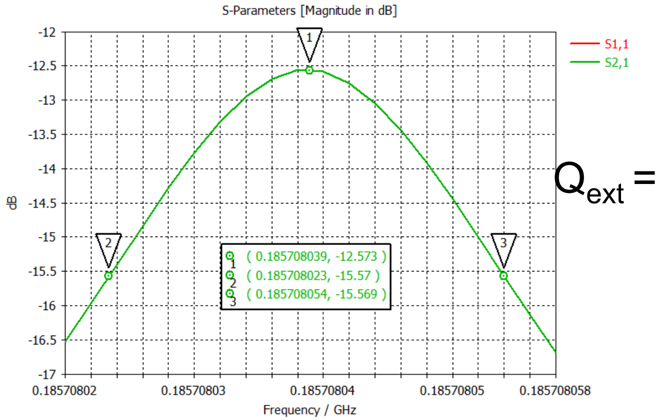


$Q_{ext}$ = 6.0e6

- Time-domain Solver
  - Measure a decay time of the stored energy and calculate $Q_L$. Then $Q_{ext} = Q_L$

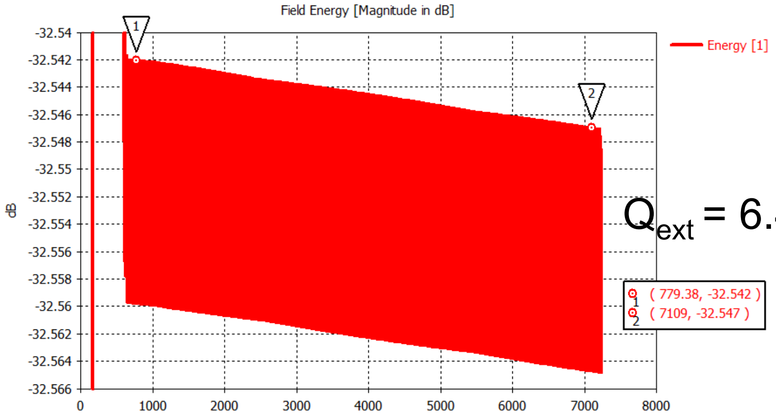


$Q_{ext}$ = 6.4e6


[100] V. Shemelin, S. Belomestnykh, "Calculation of the B-cell cavity external Q with MAFIA and Microwave Studio," SRF020620-03

# Coupling Strength Adjustment

## Example: LCLS-II-HE SRFgun cavity FPC [19]

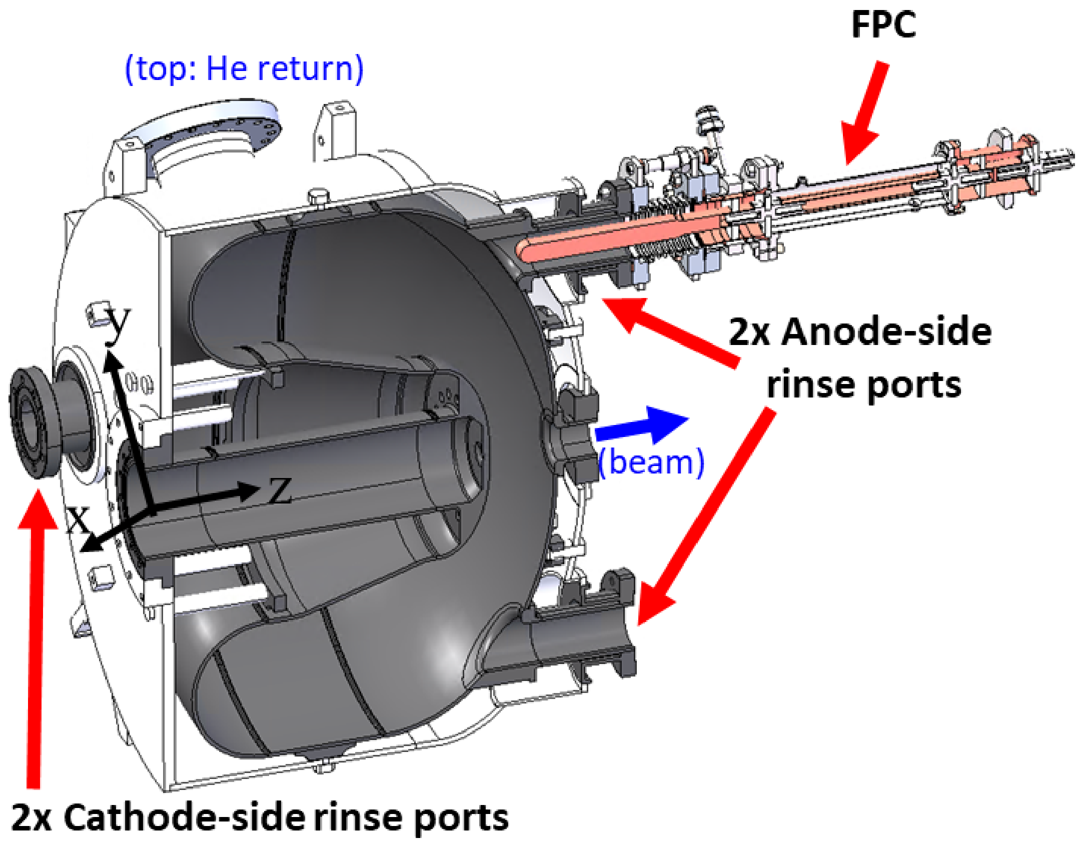


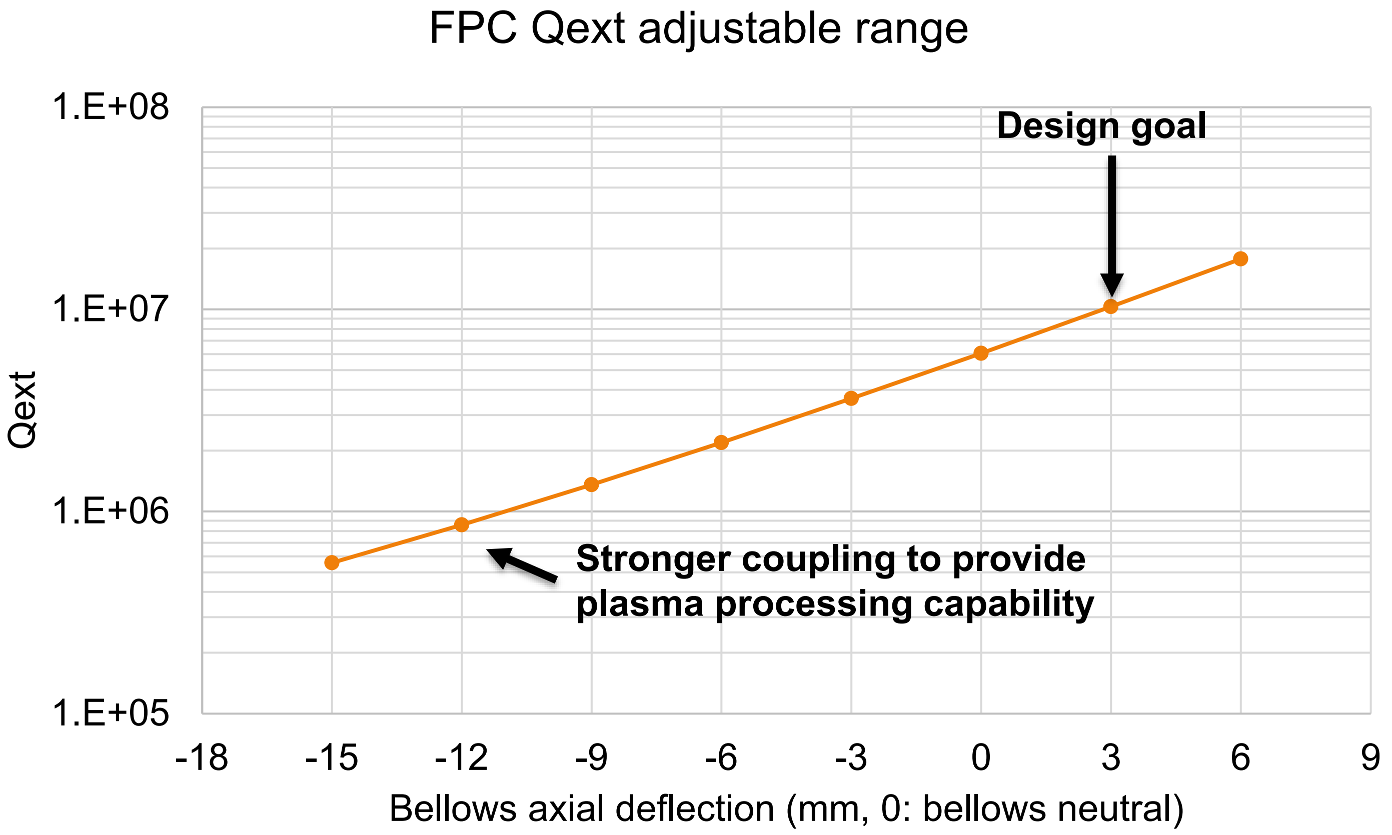



[19] S. Kim et al., "Design of a 185.7 MHz Superconducting RF Photoinjector Quarter-Wave Resonator for the LCLS-II-HE Low Emittance Injector," Proc. NAPAC2022, p. 245 (2022).

# Impedance Matching in a RF Window

- Characteristic impedance in a coax line:

$$Z_0 = \frac{1}{2\pi}\sqrt{\frac{\mu}{\epsilon}}\ln\left(\frac{D}{d}\right)$$
$$\cong \frac{60\Omega}{\sqrt{\epsilon_r}}\ln\left(\frac{D}{d}\right)$$

- A tapered transition for impedance matching with a planar ceramic window
- At low frequencies, a tapered transition is often not necessary

**APS-U 1.4 GHz higher harmonic cavity FPC:**
**Conical transition in RF window**
**(Courtesy of M. Kelly and S. Kutsaev [1])**

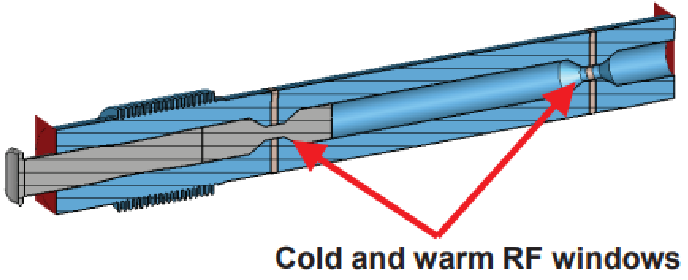


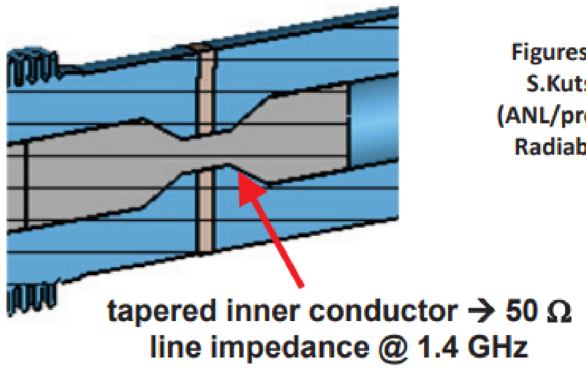


Figures from S.Kutsaev (ANL/presently Radiabeam)

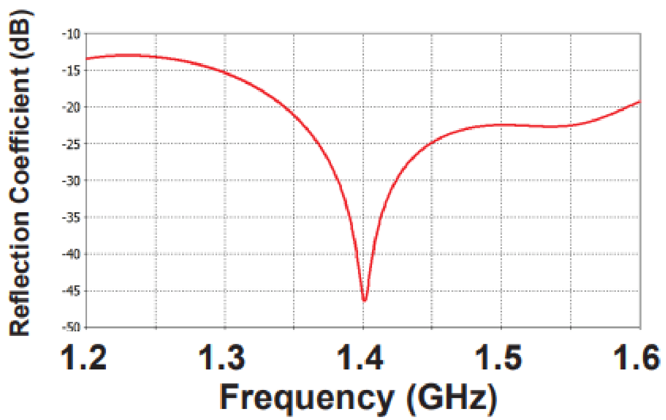

# Impedance Matching in a Two-Window Coupler

- In a two-window coupler, impedance matching depends on the distance between windows as well

**FRIB Energy Upgrade 644 MHz FPC:**
**No conical transition in RF window (relatively low frequency)**
**Distance between two windows are critical**

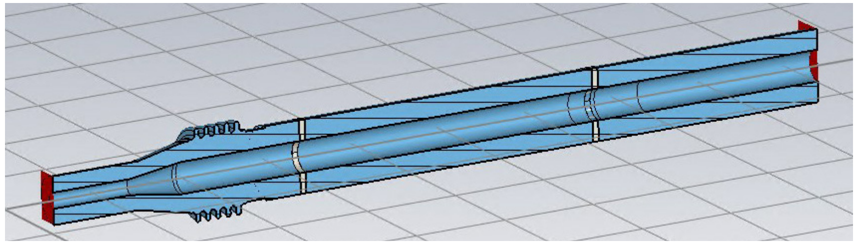

**Impedance matching changes with respect to window-to-window distance**

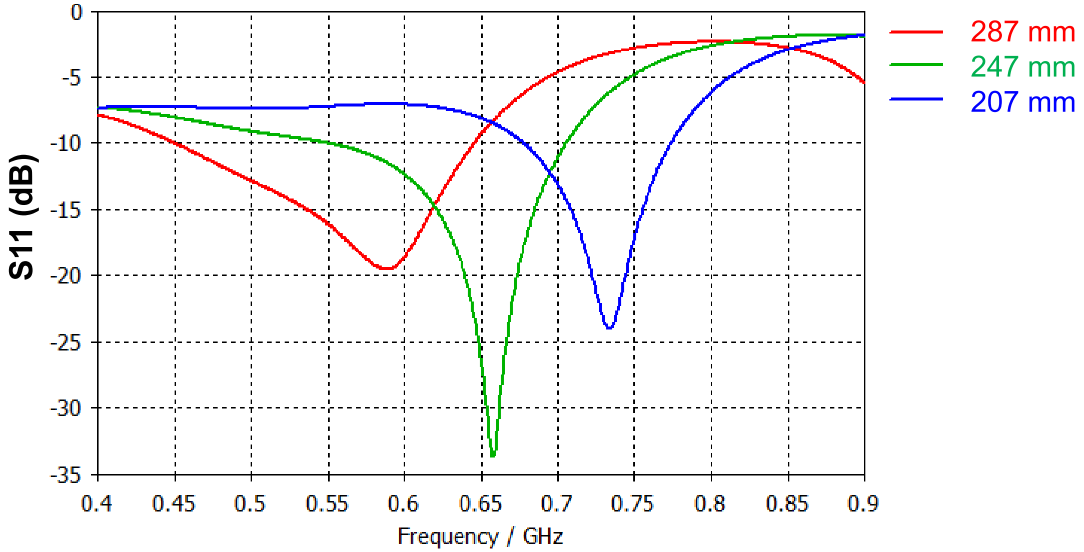

# RF-Thermal Simulations to Calculate Total Heat Load

**Example: PIP-II 162.5 MHz HWR FPC (Courtesy of M. Kelly, S. Kutsaev [1])**

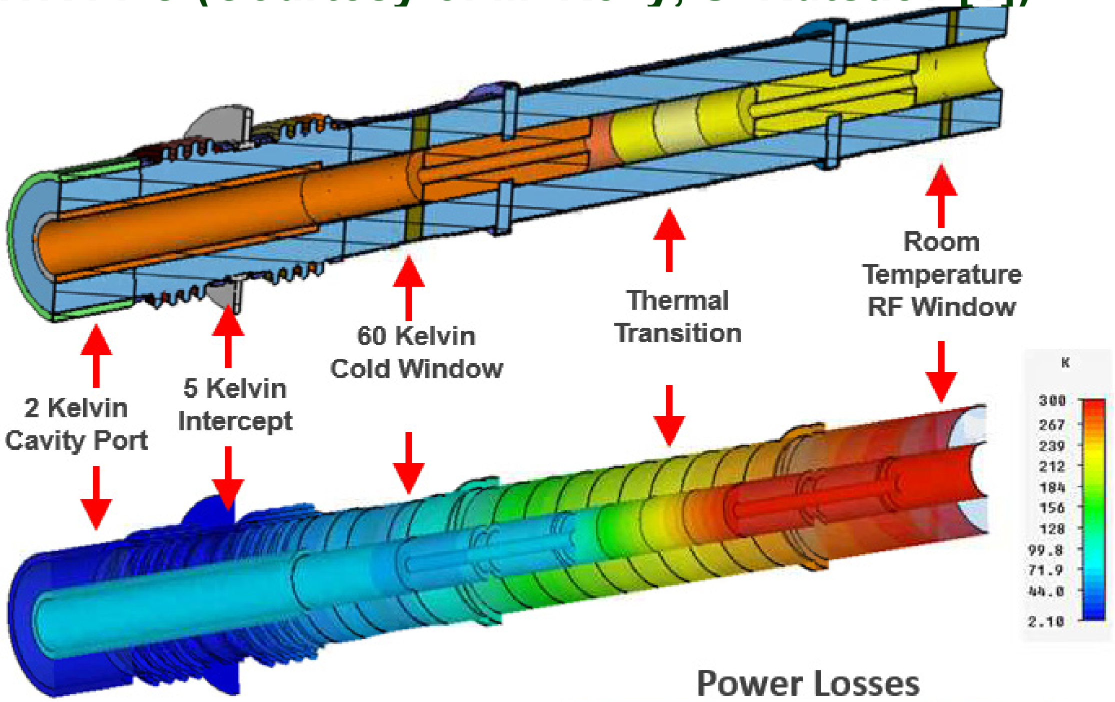


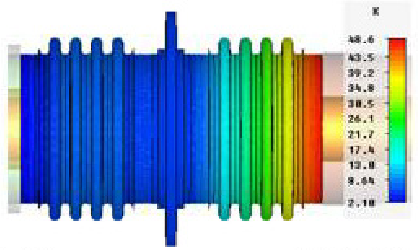


### Power Losses

| Parameter | Value |
|---|---|
| Input Power, kW full reflection | 15.0 |
| Power Flow to 2K, W (total) | 0.165 |
| Power Flow to 5K, W (total) | 2.49 |
| Power Flow to 60K, W (total) | 11.8 |
| Power Flow to 2K, W (static) | 0.057 |
| Power Flow to 5K, W (static) | 1.58 |
| Power Flow to 60K, W (static) | 2.59 |

*Modern FEM codes support to find a self-consistent solution with temperature-dependent electrical and thermal conductivities*

# Practice to 'Manually' Find a Self-Consistent RF-Thermal Solution

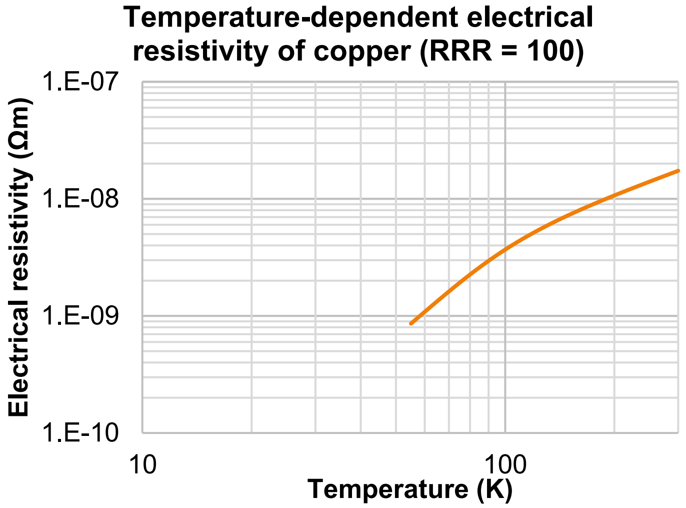


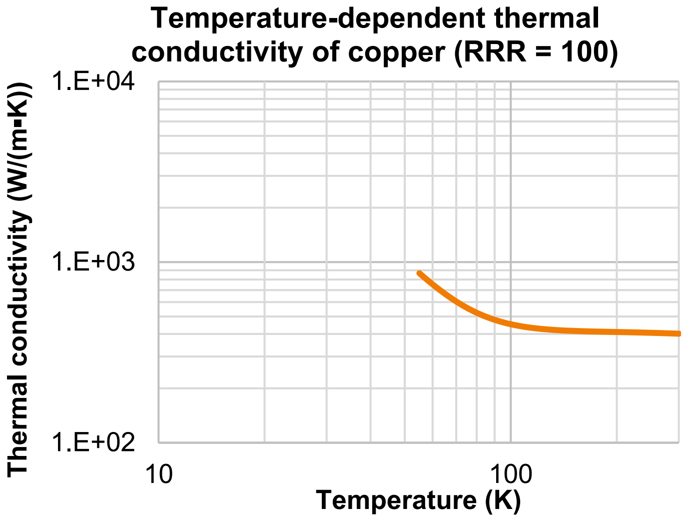


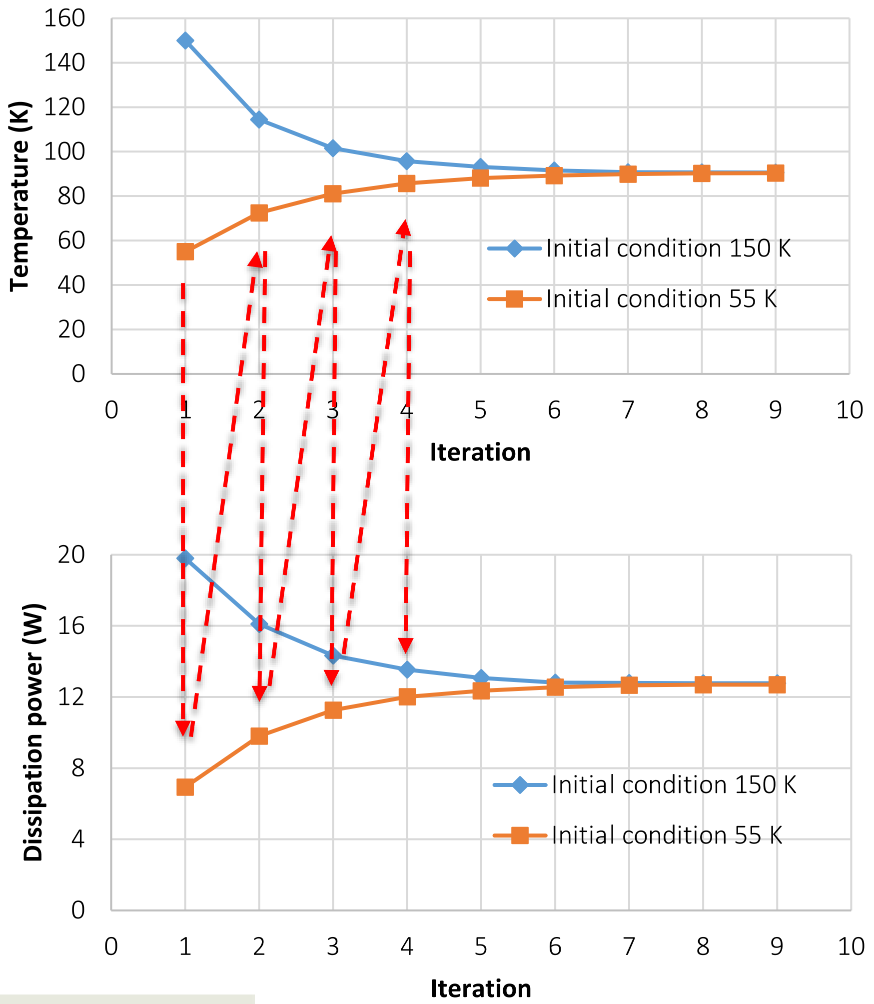


## Self-consistent solution: 91 K with 12.7 W

A dominant source of the heat load is cavity H-field at the antenna tip in this coupler

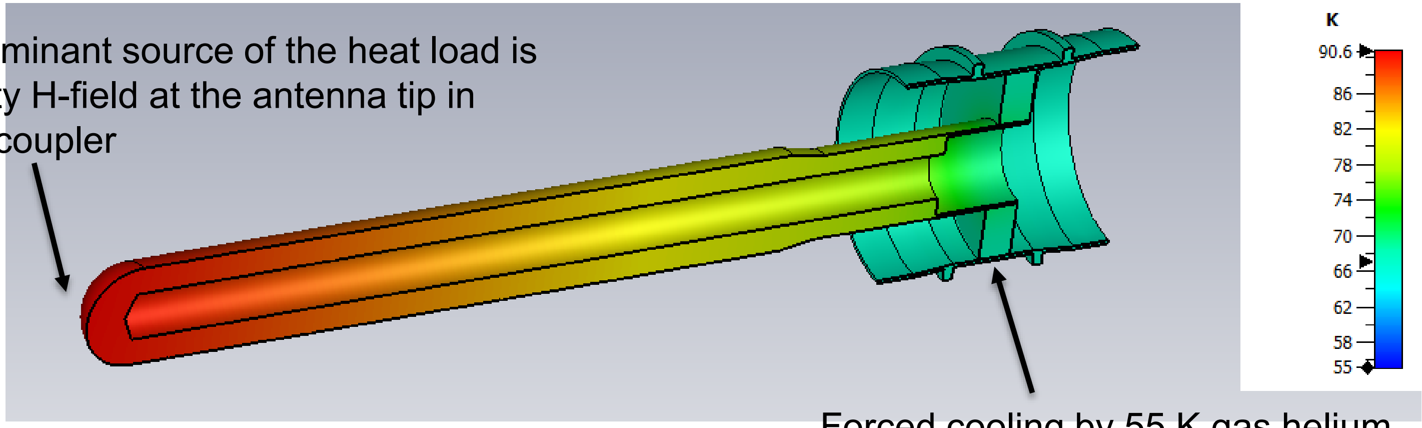


Forced cooling by 55 K gas helium

# Multipacting Simulation

Example: FRIB 322 MHz FPC integrated with β=0.53 HWR using CST PIC Solver with MWS

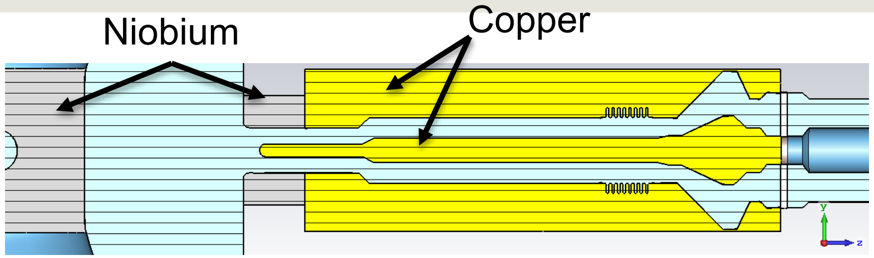


**Motivation**: in cryomodule tests, observed MP threshold changes with the detuning

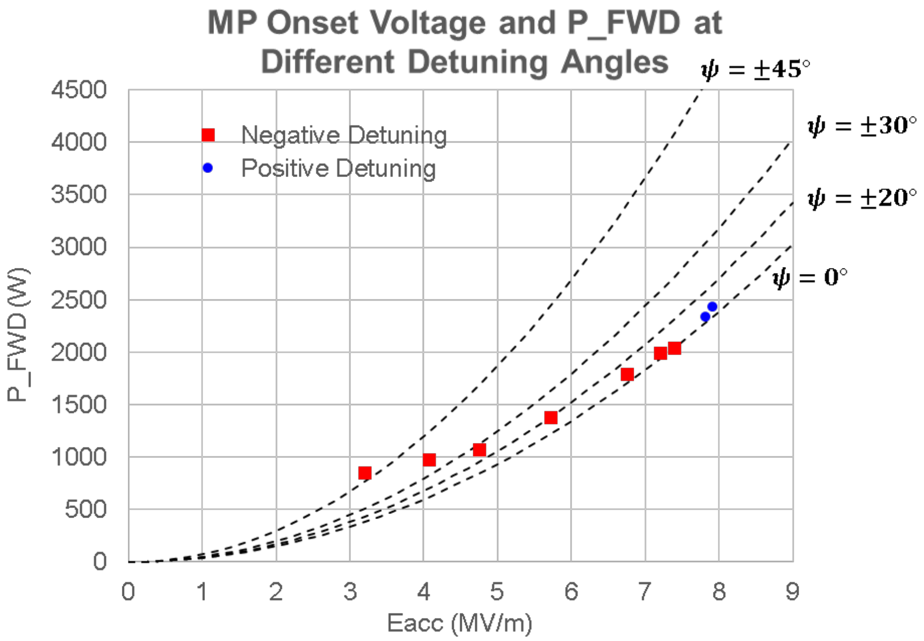


**E-field from CST MWS FD Solver**

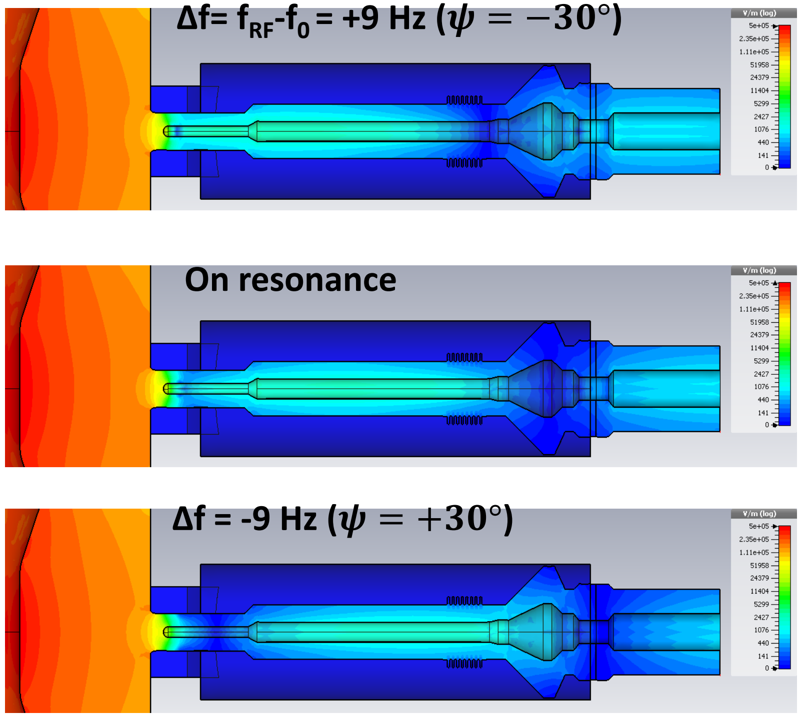


Seed electrons: 12 or 18 bunches uniformly spaced in one RF period

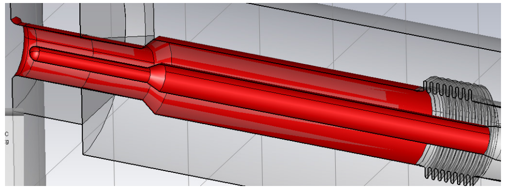

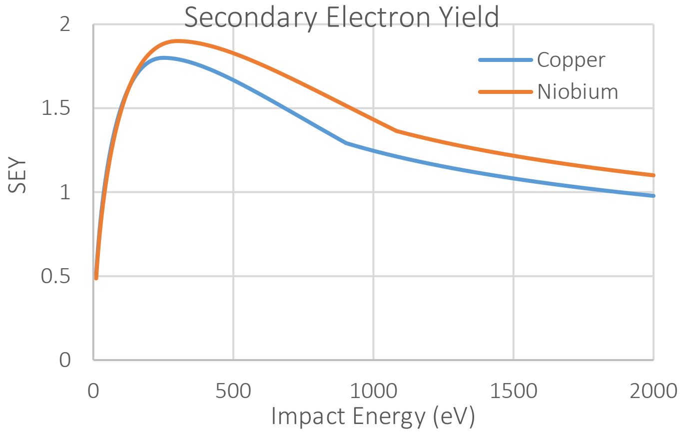

# Multipacting Simulation (continued)

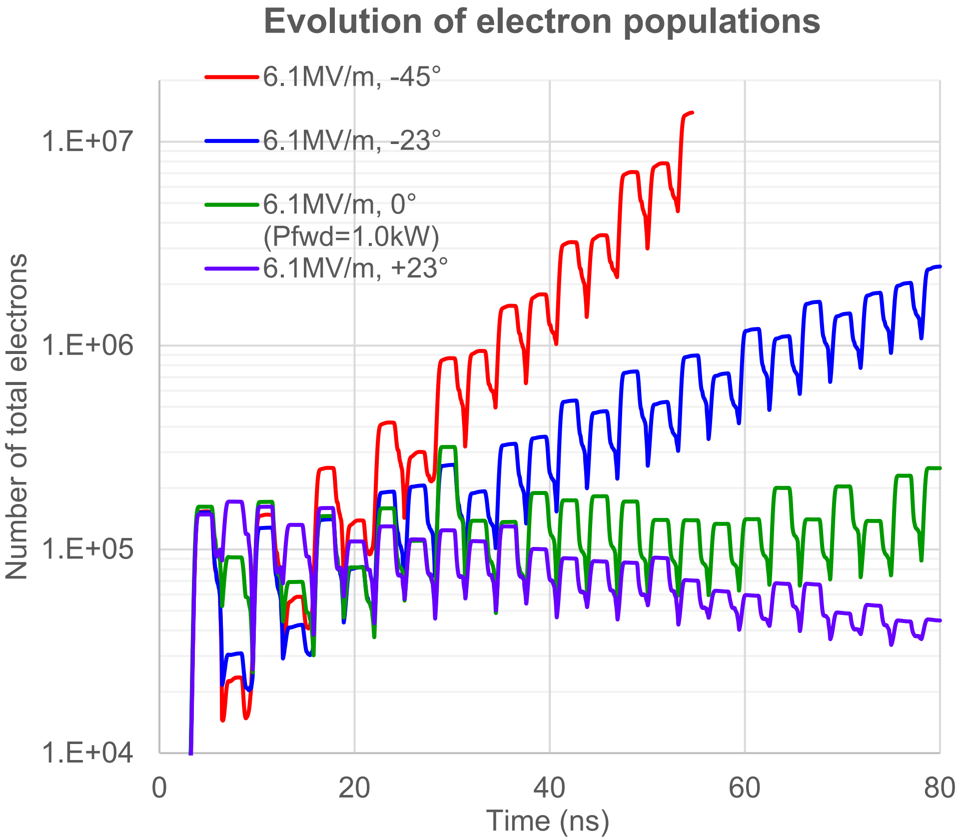


Simulated MP growth rates are roughly consistent with measurements

**Movie: motion of electrons**

Time frame: from 22.5 to 25.75 RF cycles
Number of particles: 1 to 2 millions

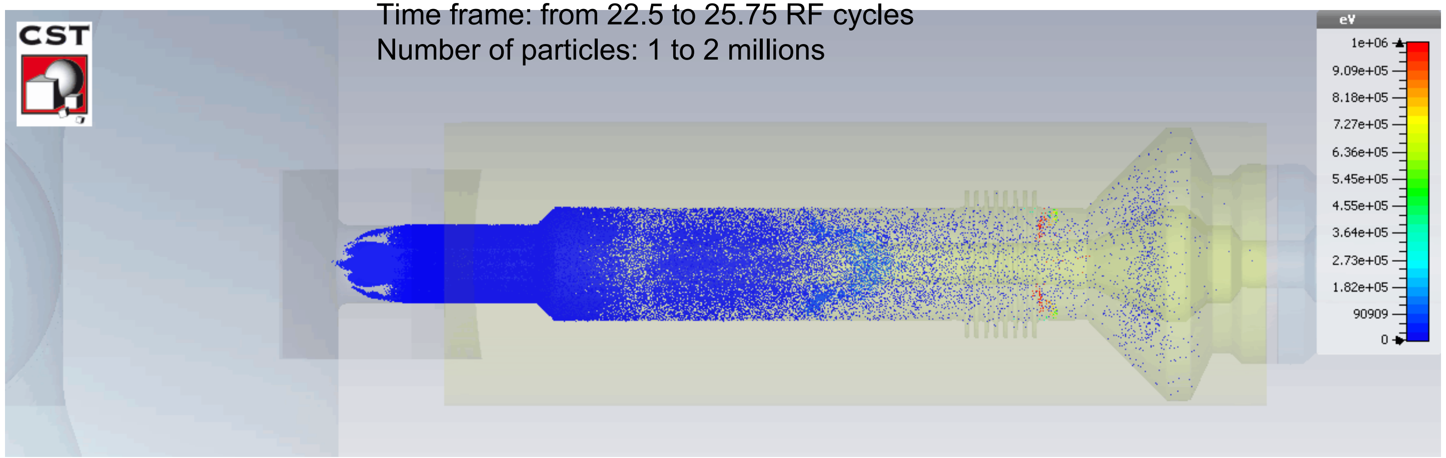


- Particle tracking shows MP location is as expected
- More importantly, a potential dangerous mode of coupler MP: If coupler MP appears near the cavity, electrons can gain energy from cavity E-field. Such "high-power" electrons will be deposited to cavity or coupler surfaces which can cause: 1) **cavity quench**, 2) **coupler unexpected heating**, 3) **radiation damage of ceramic window,** if not shielded by coupler metallic structures

# Coax Multipacting Band and Suppression by DC Bias

ANL's 162.5 MHz FPC for PIP-II HWRs (Courtesy of M. Kelly [1])

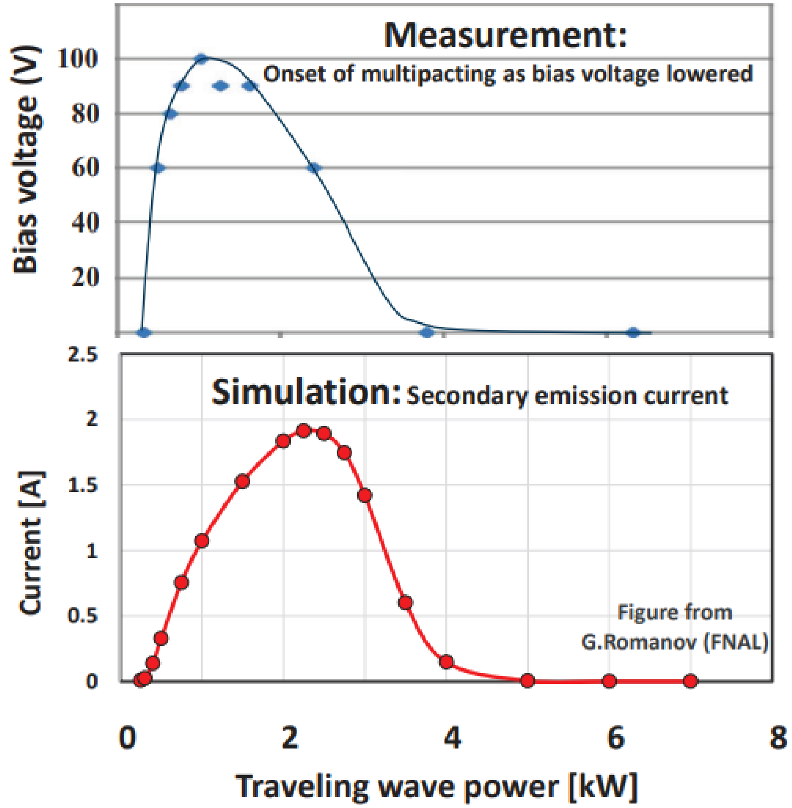


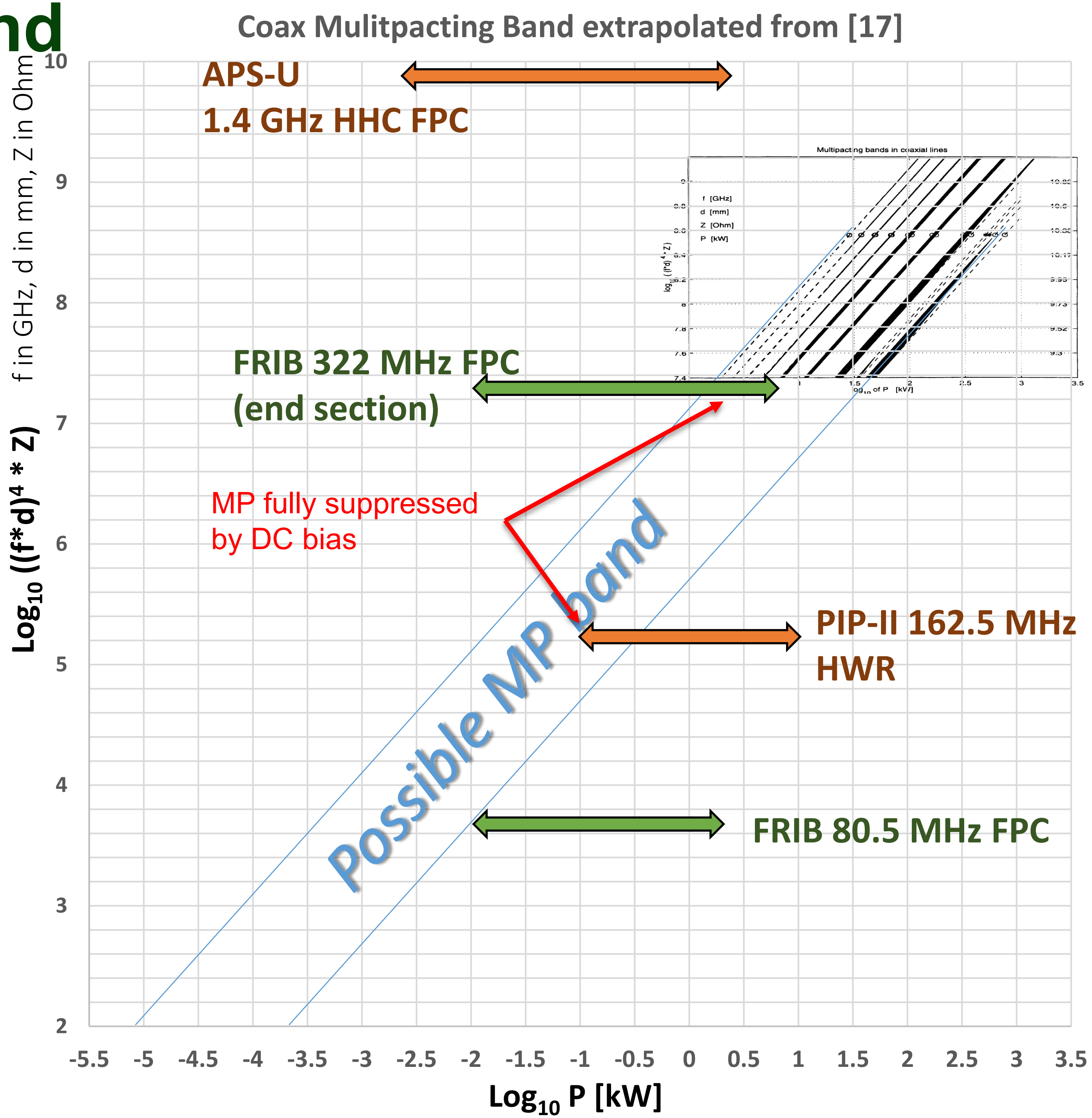


[17] E. Somersalo et al., "COMPUTATIONAL METHODS FOR ANALYZING ELECTRON MULTIPACTING IN RF STRUCTURES," Particle Accelerators, Vol. 59, pp. 107-141.

# Design Consideration: Cavity Field Emission

- Concerns: radiation damage of ceramic window due to cavity field emission electrons, if cavity is 'dirty'
- Can be considered in design
  - Example: LCLS-II-HE SRFgun with a planar ceramic window as a 'cold' window

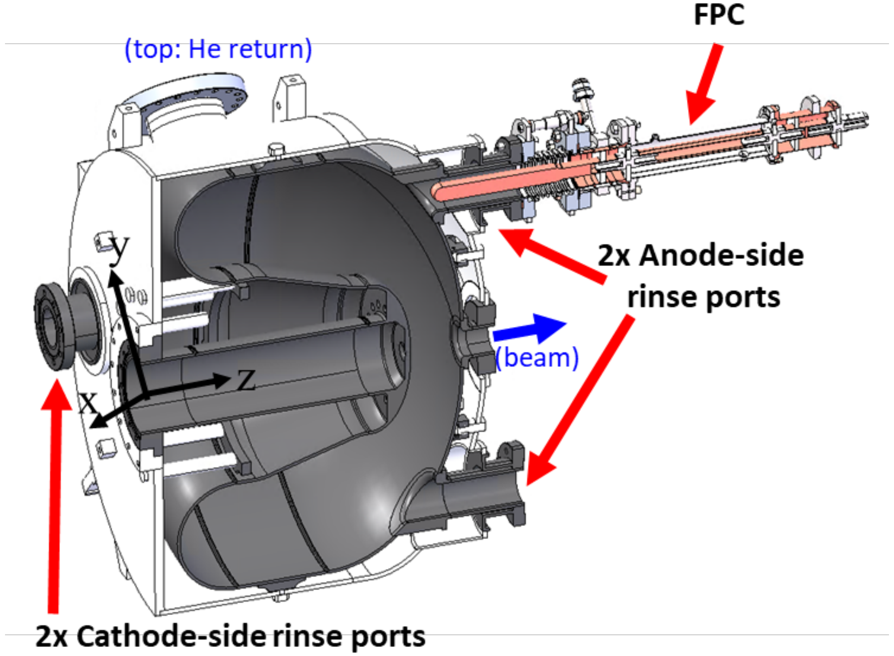


$\phi = +30^\circ$

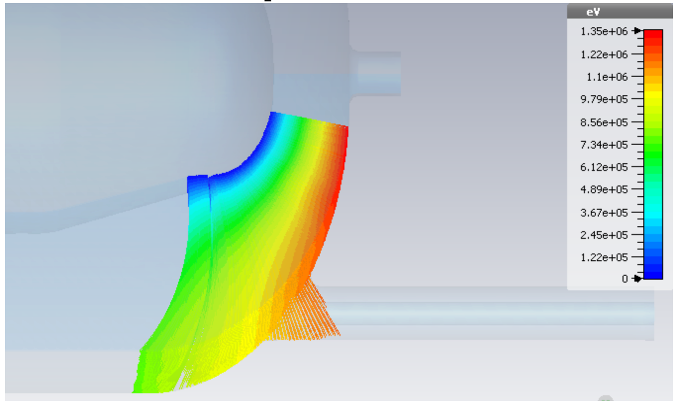


$\phi = 0^\circ$

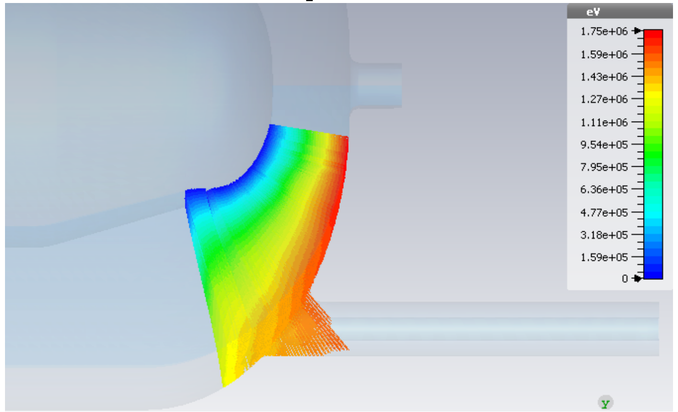


$\phi = -30^\circ$

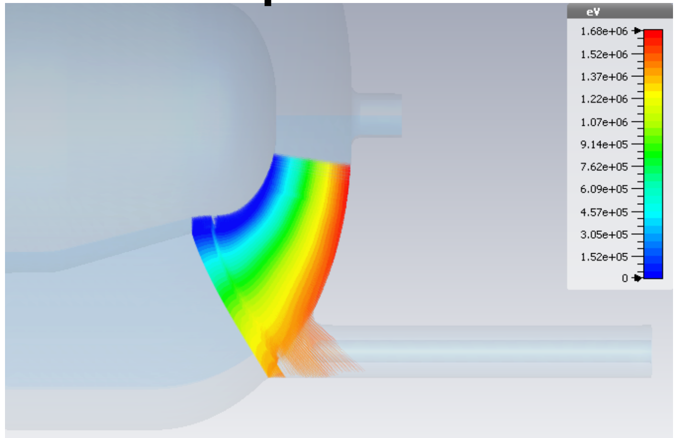


$\phi = -60^\circ$

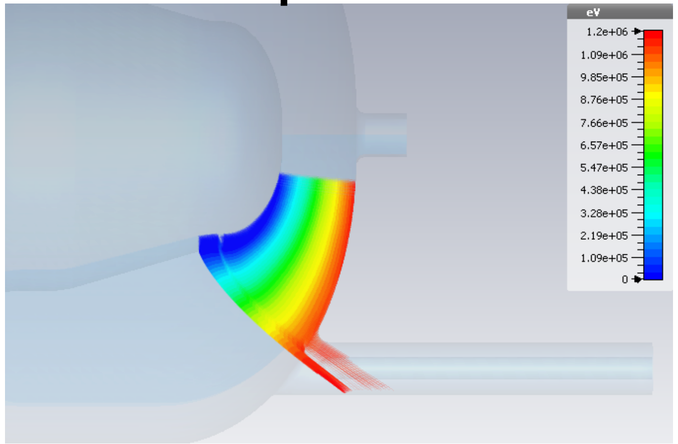

# High-pass Filter in HOM Couplers

Example: a conceptual HOM coupler for a QWR

**A 117 MHz QWR with 4 HOM couplers**

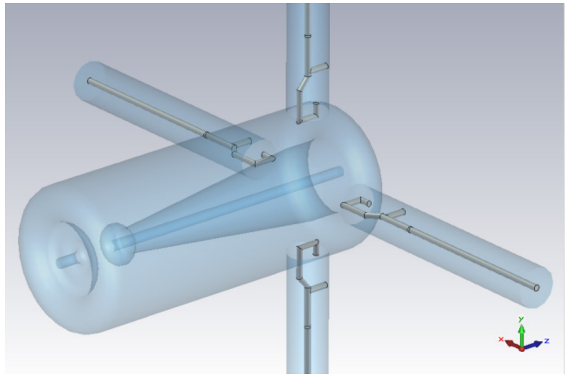

**LC high-pass filter**

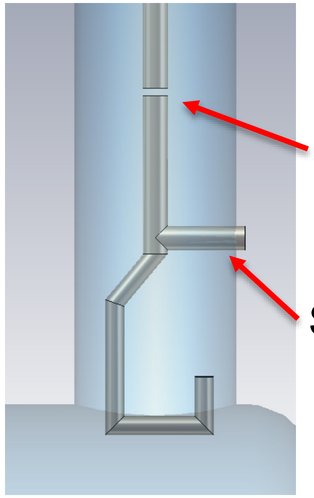

gap: capacitance

Short-to-ground: inductance

*Complexity of HOM couplers: this short needs to be niobium*

FM: well confined

HOMs: well extracted and thus damped

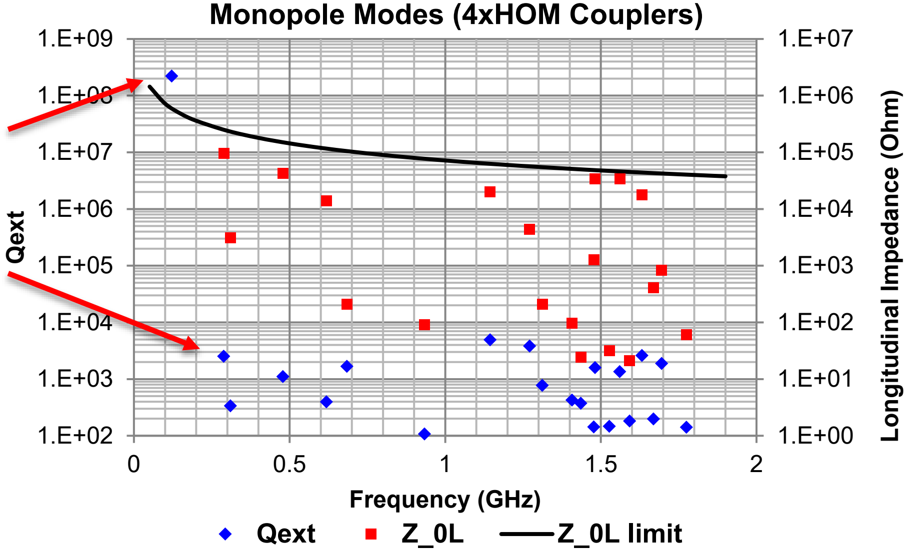


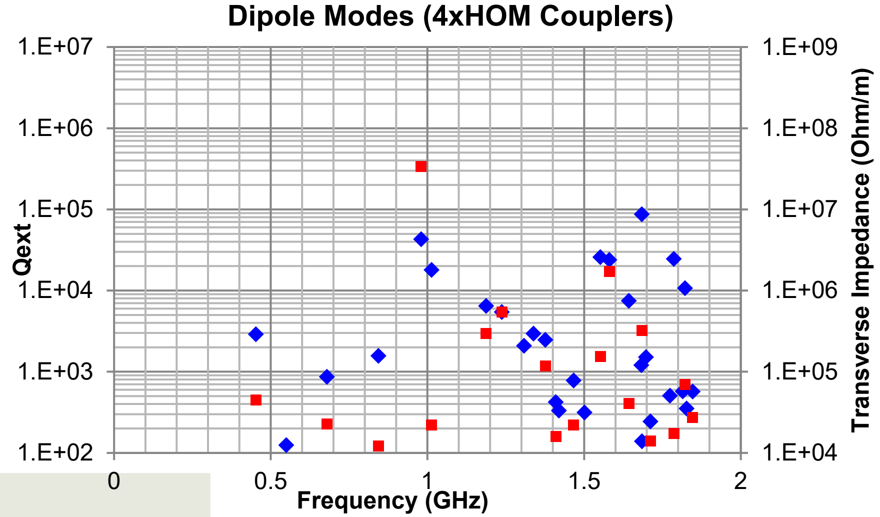


*For more information about HOM impedances, please see the next lecture*

# Coupler-Induced HOM and Its Mitigation

- In APS-U 1.4 GHz HHC system,
  found a harmful HOM induced by coupler in the original design
- The wedge antenna allows to extract the HOM via TEM mode and thus strongly damp the HOM

**Symmetric Antenna**

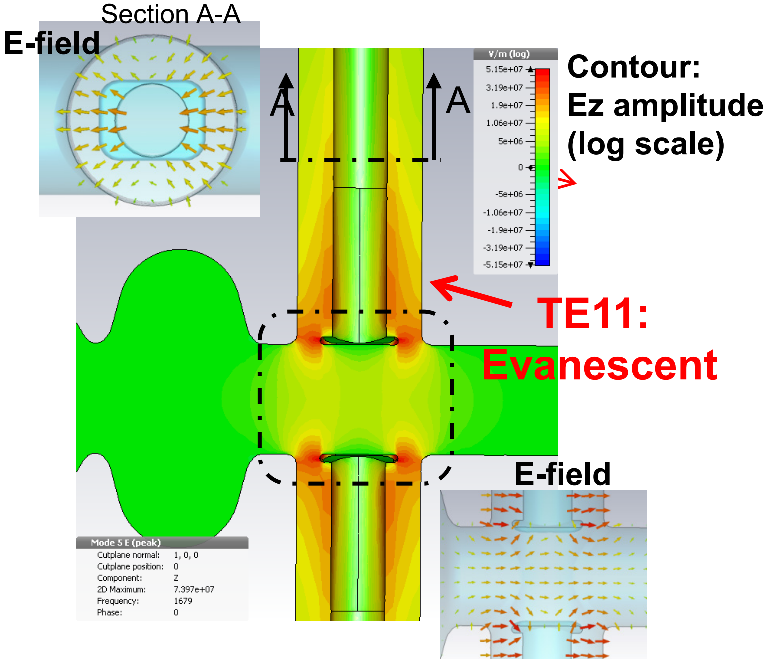


**Asymmetric Antenna**

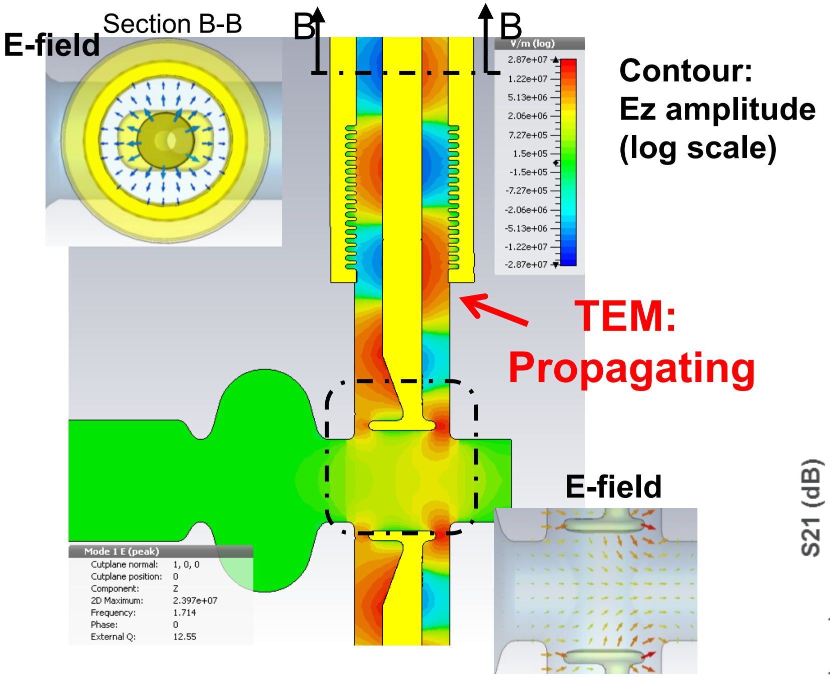


**Symmetric Antenna** **Wedge Antenna**

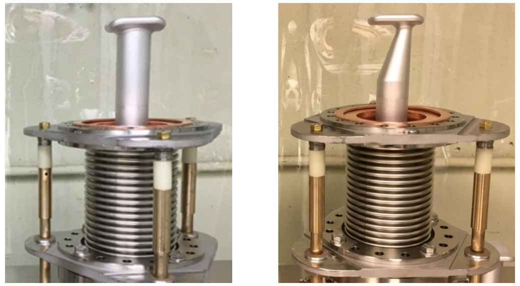

**Coupler Mode Measurement at Room Temperature**

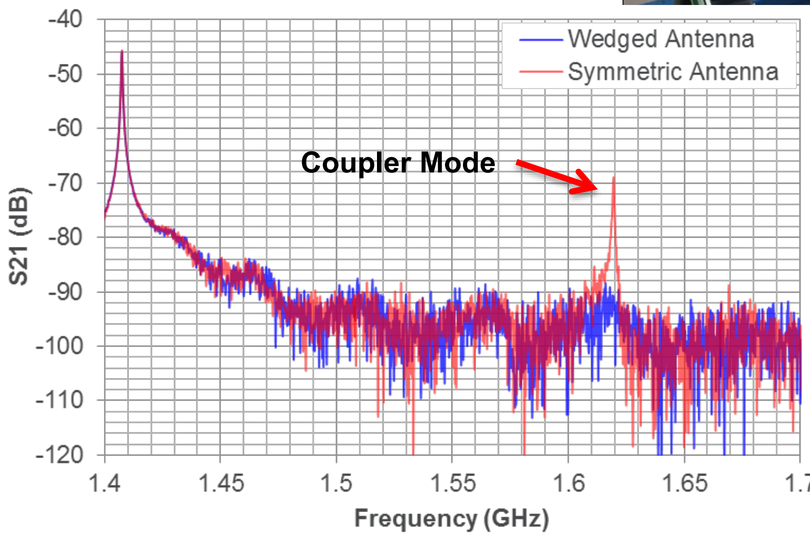

# Fabrication, Preparation, Assembly

- RF window: ceramic brazing, TiN coating
- Cold bellows, thermal transitions: copper plating
- Cleaning, baking, clean assembly

# Ceramic Brazing to Copper
## (very brief introduction)

- Design considerations for ceramic brazing
  - Options
    - » Metallization, e.g. Moly-manganese
    - » Active metal brazing, e.g. AgCuTi alloy
  - Metal selection: metals with a low elastic modulus and/or a low yield strength to reduce residual stress in the braze joint, caused by differential CTE upon thermal cycle during brazing
  - Alloy selection: the two adjoining surfaces must be "wettable"
  - Mechanical design to mitigate different CTE
- Additional consideration for cold window
  - Thermal cycle induced fatigue life

SEM images of cross-section at brazed joint [20]

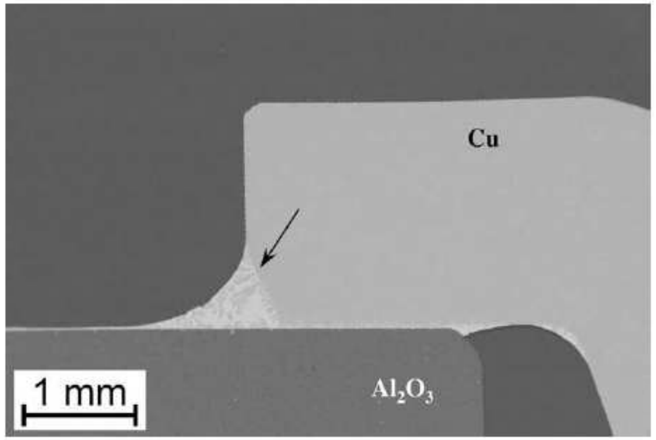


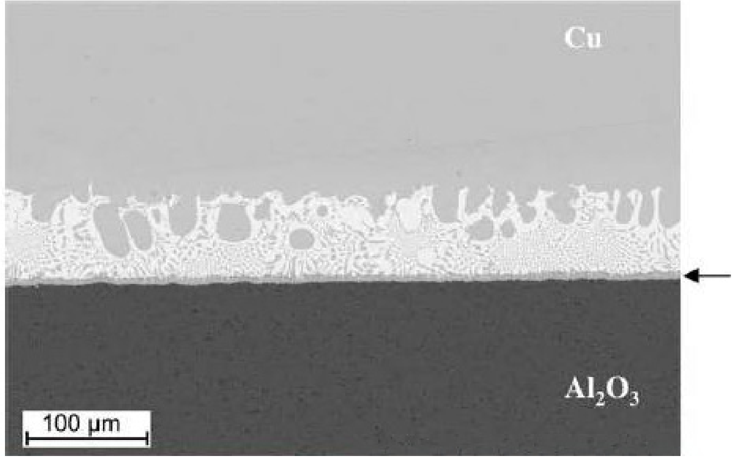


[20] O. Kozlova et al., "Brazing copper to alumina using reactive CuAgTi alloys" Acta Materialia 58 (2010) 1252.

# Analysis of Fatigue Life upon Thermal Cycles

Example: Cold window of ANL 162.5 MHz coupler for PIP-II HWR (courtesy of M. Kelly [1])

**Brazed alumina into OFHC copper has a finite fatigue life when cycled to 80 K**

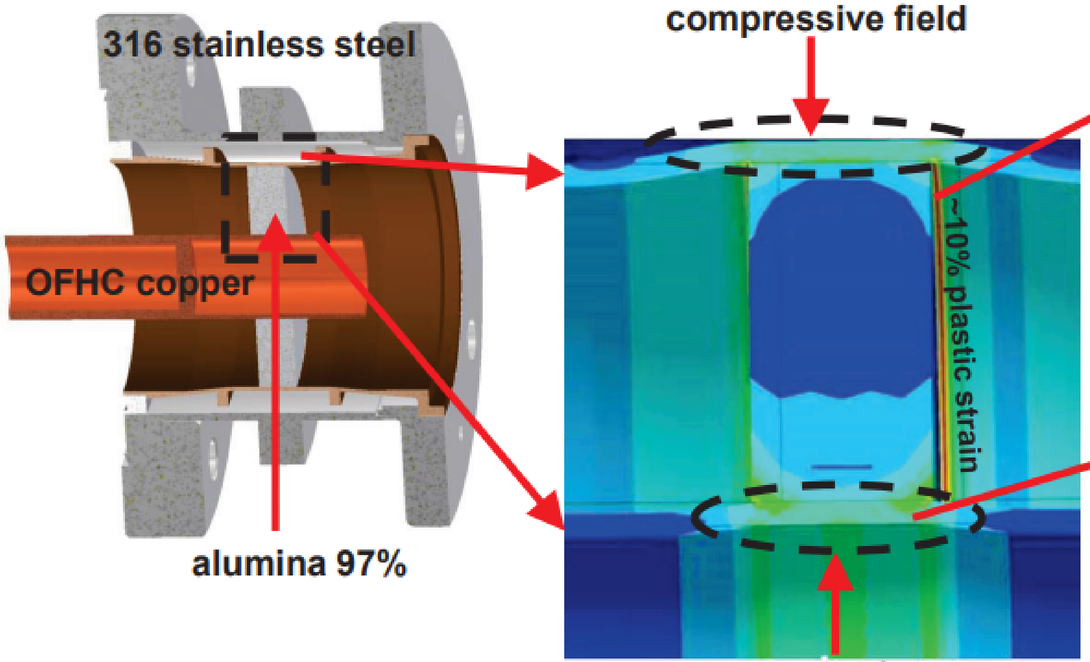


Figure from R.Fischer (ANL)

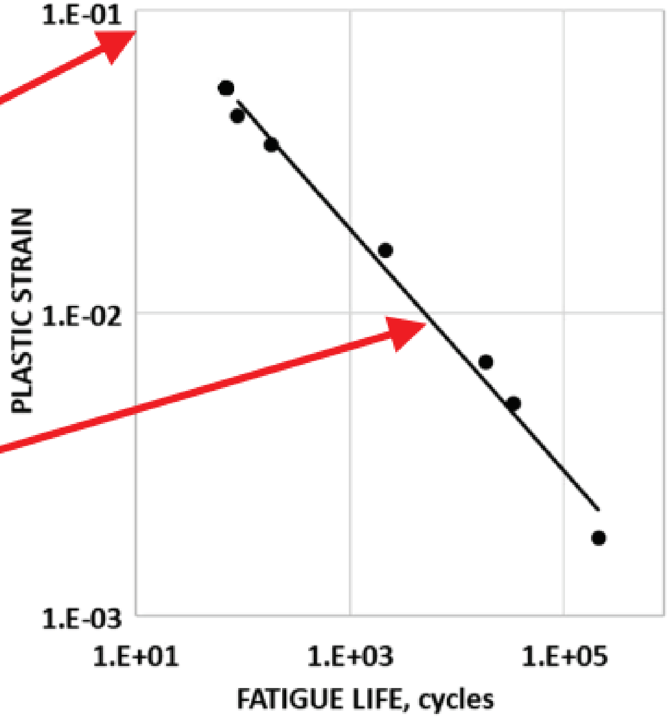


- Copper/alumina brazing cycle down to 80 K produces ~1% plastic strain → finite lifetime
- Corners can produce much higher local values, ~10%
- Chamfered or radiused corners on the ceramic with a meniscus of braze alloy mitigate local stresses/strains (experimentally several units cycled up to 100 times with no issues)

# Thermal Conductance at Ceramic-to-Copper Brazed Joints

APS-U 1.4 GHz HHC FPC cold window [1]: 97% alumina planar ceramic window brazed onto both inner and outer conductors

Thermal conductivity of 97% alumina was close to the literature value 100 W/(m·K) and no additional contact resistance was found

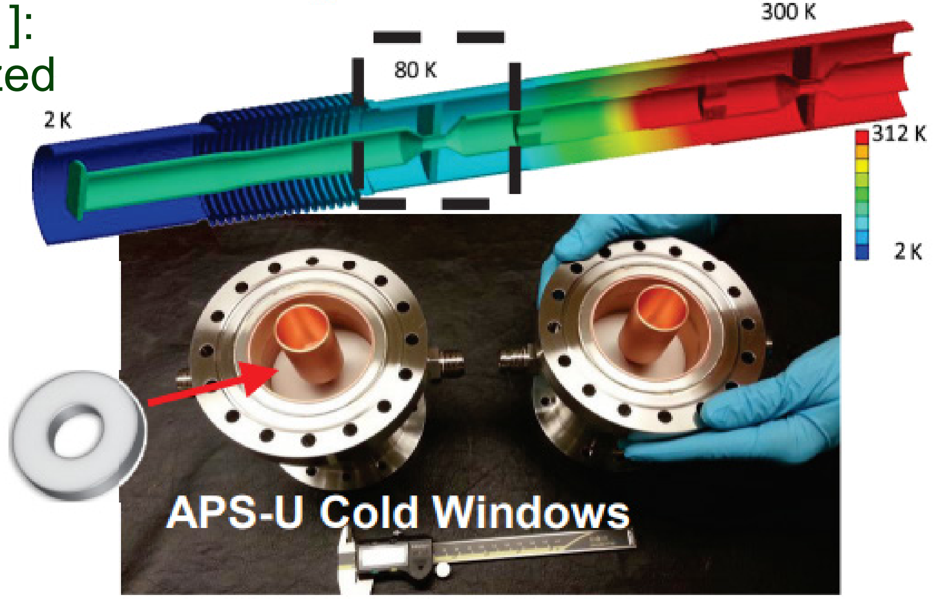


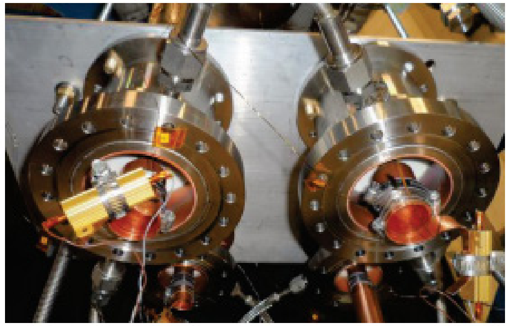

80 K test apparatus

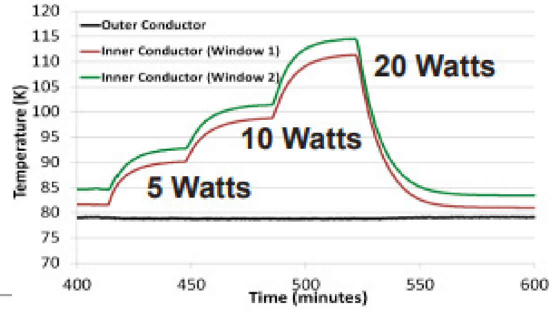


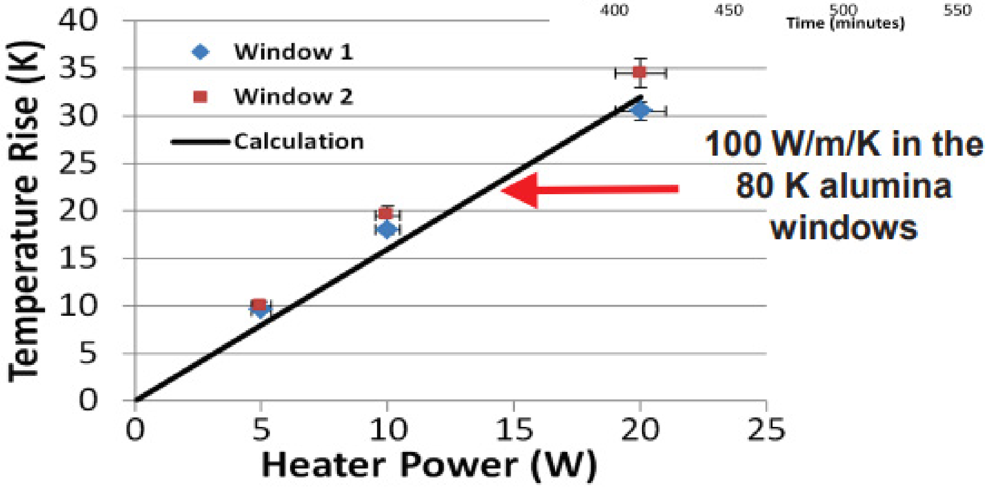

# Cold Shock and Vacuum Leak Check

- Thermal cycles with liquid nitrogen is turned out to be useful process to find potential leaks at the brazed joints of cold window: QA procedure
- Light oxidation of the copper surfaces: acidic detergents such as Citranox are turned out to be useful to remove such oxides

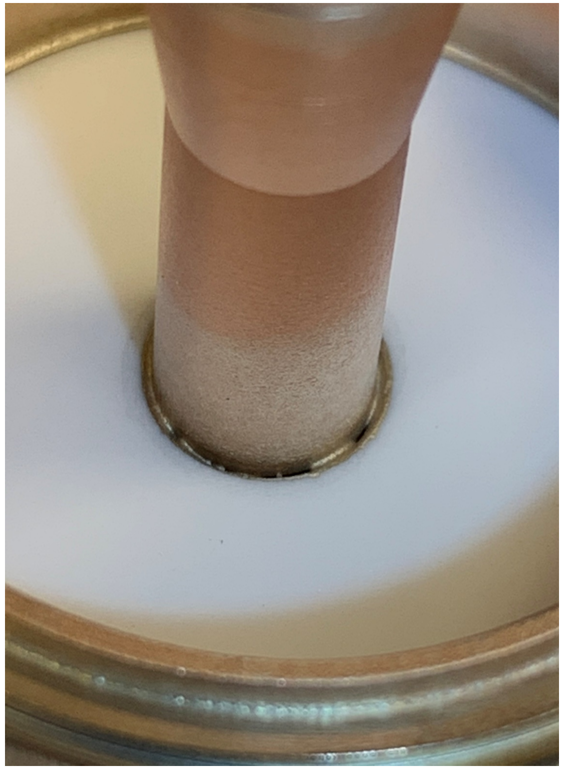

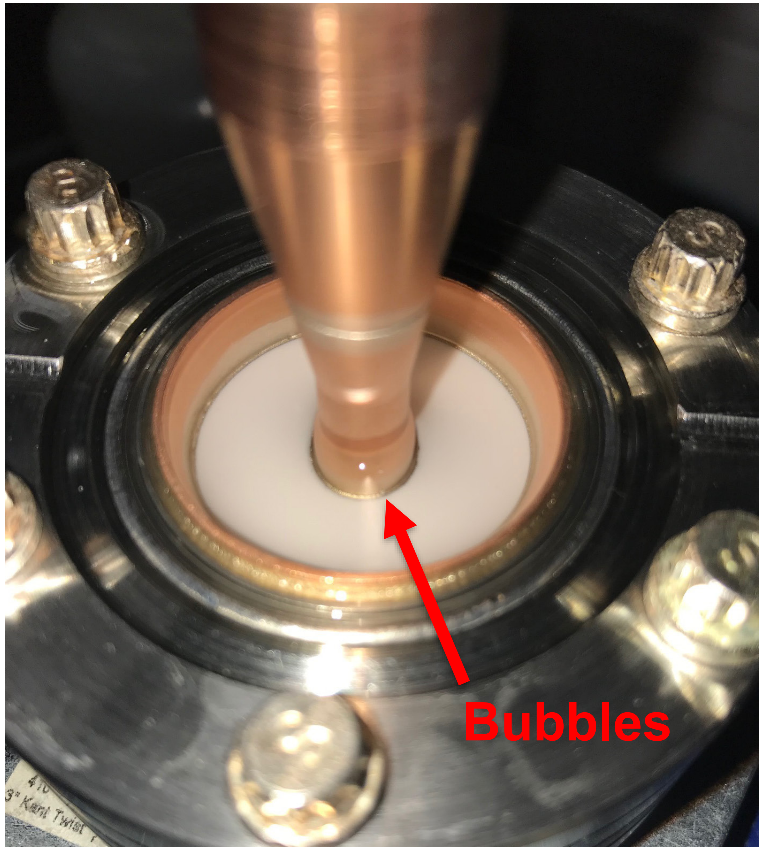

# Titanium Nitride Coating on Ceramic Window
## (very brief introduction)

- High SEY of alumina compared to the other material
- Very thin layer (1-2 nm) metal coating to reduce SEY: TiN widely for chemical stability
  - Need to be thin to avoid excessive heating
- Methods
  - Sputtering
  - Evaporation
- Note
  - Developed for high-power pulsed (~100 MW a few us) S-band klystron RF windows: necessary to avoid MP-induced RF breakdown
  - Found to be also useful/critical for high-power SRF FPCs
  - Not observed MP in FPCs with planar ceramic windows operated at CW ~10 kW or less while windows are not TiN coated (FRIB 80.5 MHz and ANL): may depend on possible MP trajectories

SEY of insulator material and TiN [21]

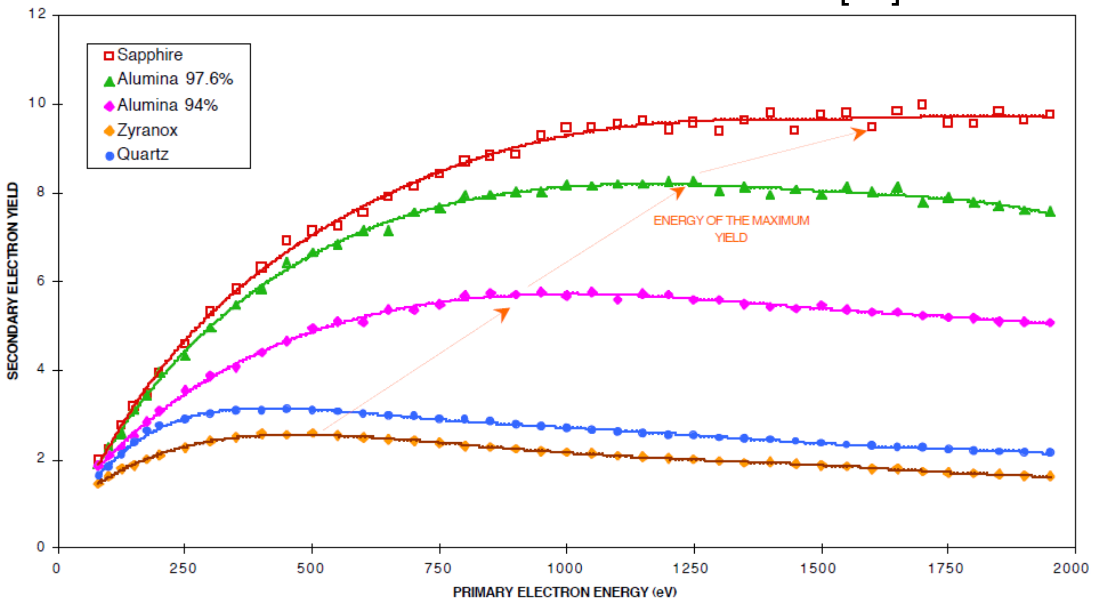


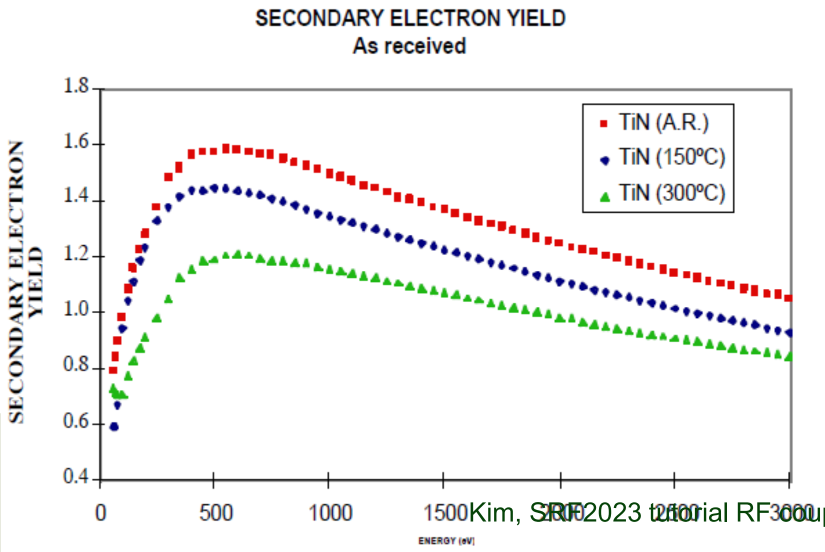


[21] N. Hilleret, "Surface properties of technological materials and their influence on the operation and conditioning of rf coupler," HPC Workshop (2002).

# Copper Electroplating
## (very brief introduction)

- Methods [22]
  - Acid copper sulfate, pyrophophase copper, cyanide/cyanide-free copper
  - Additives are necessary as ‘accelerator’, ‘suppressor’, ‘leveler’ [23]
  - Example of process [24]
    - » Assembly of the anode and jig > electrolytic degreasing > rinsing > activation of 316L SS substrate > rinsing > 0.5 um Ni or Au strike > rinsing > 20 um copper plating > rinsing > disassembly of the anode and jig > rinsing > drying
- As a SRF cavity component, it is required:
  - No degradation of electrical and thermal conductivities compared to bulk copper
  - Particulate clean
  - High RRR is favorable

**Copper electroplating with copper sulfate [23]**

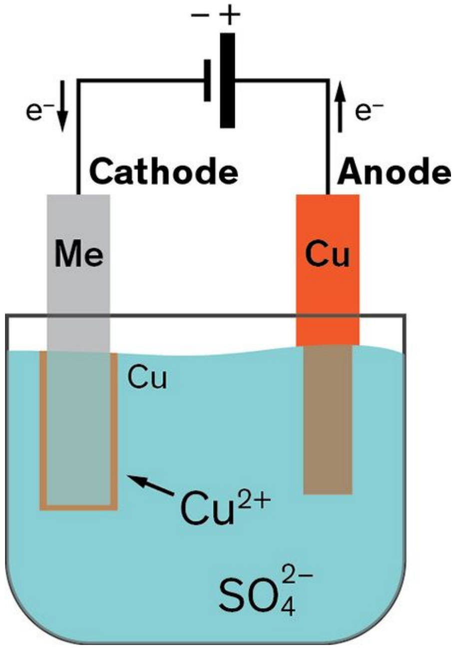



[22] J.W. Dini, D.D. Snyder, “Electrodeposition of Copper,” Modern Electroplating (2010 John Wiley & Sons, Inc.) pp. 33-77.
[23] https://www.dupont.com/blogs/copper-electroplating-fundamentals.html
[24] H. Kutsuna, T. Ikeda, “Quality control of copper plating for coupler (at Nomura Plating),” LCWS13 (2013).

# RRR of Copper Plating

- RRR depends on the details of electroplating process
  - Reported RRR is affected by microstructure such as the grain size [25]
- Heat treatments change RRR: improved at ‘medium’ temperature but degraded at ‘high’ temperature [14]
  - Possible cause: grain structure improved initially at mid-T’s but nickel diffused to near surface at high temperatures
- Ultra high RRR may not be needed as the RF surface resistance at cryogenic temperatures could be limited by anomalous skin effects; it depends on the frequency

RRR changes after baking [14]

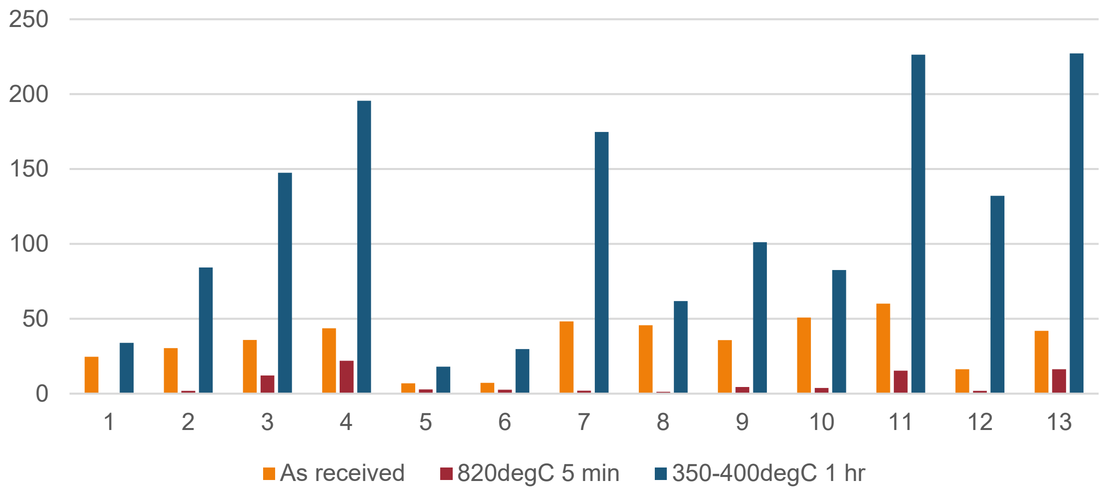


**Grain size [25]**

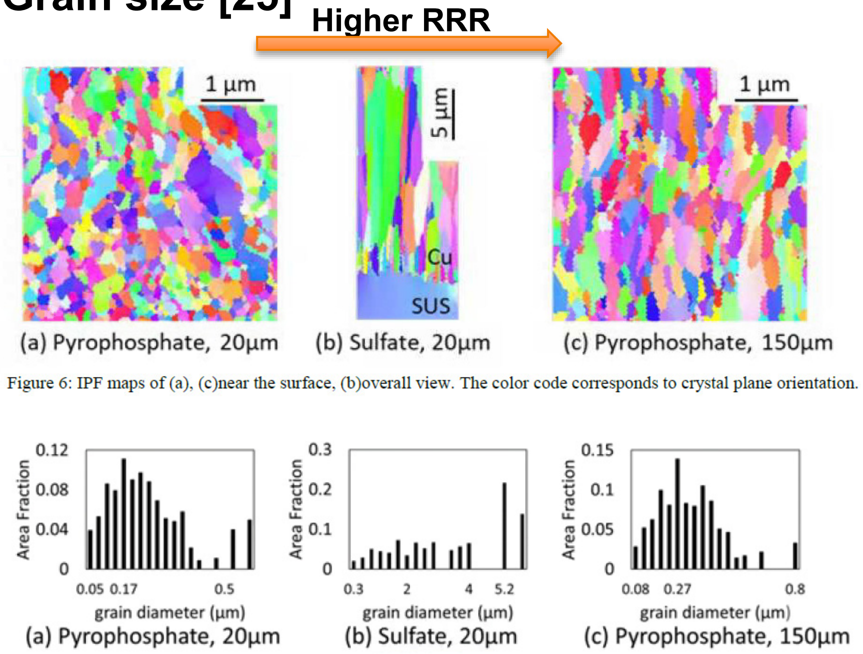



[14] W. Signer, D. Dwersteg, “Influence of heat treatment on thin electrodeposited cu layer,” Proc SRF’95, p. 653 (1995).
[25] Y. Okii et al., “R&D of Copper Electroplating Process for Power Couplers: Effect of Microstructures on RRR,” Proc. SRF2019, p. 279 (2019).

# Cleaning and Clean Assembly

- Since FPC is assembled with a cavity, particularly the antenna is inserted into a high E-field region, **degreasing and particulate cleaning** is critical to keep the cavity performance
- Cleaning process following to SRF standards
  - Ceramic window assembly
    - » Degreasing with ethanol
    - » pressurized nitrogen gas cleaning
  - Copper-plated stainless steel parts
    - » Ultrasonic cleaning
    - » manual high pressure water rinse or pressurized nitrogen gas cleaning

**FRIB FPC Installation on Cryomodules in the FRIB cleanroom (Courtesy of T. Xu [26])**

**322 MHz single-window FPC**

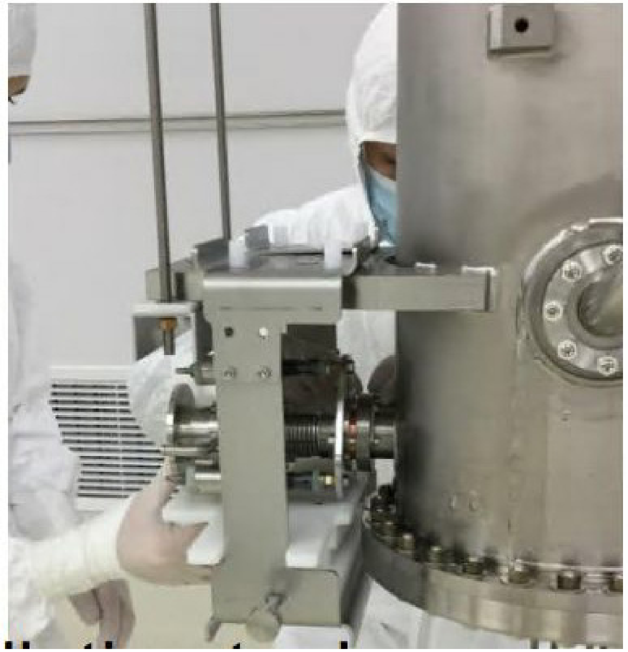

**80.5 MHz FPC cold window assembly**

[26] T. Xu, "FRIB Cryomodule Design and Production," Proc. LINAC 2016, p. 673 (2016).

# Testing and Operation

- Coupler-only high-power RF tests
- Horizontal/cryomodule tests

# Coupler High-power RF Test and Conditioning without Cavity

Common practice: FPC conditioning box in traveling wave mode ($Q_{ext1} = Q_{ext2} \ll Q_0$, $S21 = \frac{2\sqrt{\beta_1\beta_2}}{(1+\beta_1+\beta_2)} \cong \frac{2\sqrt{\beta_1\beta_1}}{2\beta_1} = 1$)

**FRIB 322 MHz FPC Test Setup [27]**

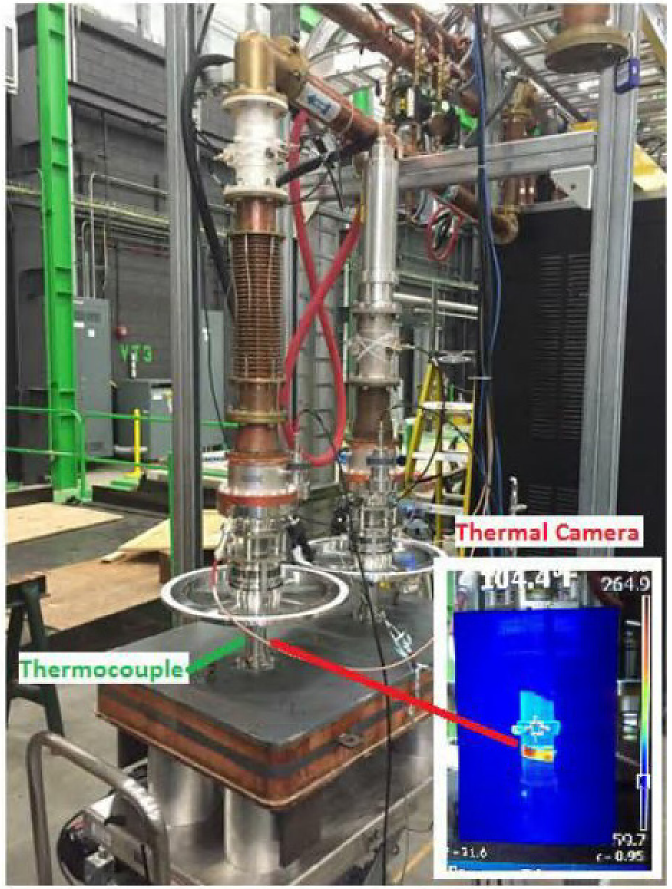


MP conditioning recipe [27]

a) Ramp up RF power from 1kW to 20kW with 0.1% duty cycle;
b) Keep 20kW RF power, ramp up duty cycle from 0.1% to 5%;
c) Keep 5% duty cycle, ramp down RF power from 20kW to 1kW;
d) Keep 5% duty cycle, ramp up RF power from 1kW to 20kW;
e) Keep 20kW RF power, ramp up duty cycle from 5% to 20%;
f) Keep 20% duty cycle, ramp down RF power from 20kW to 1kW.

- Limiting factor of RF power/duty factor ramp up is vacuum: <4e-7 Torr
- In addition, vacuum and temperature interlocks are set
  to avoid sudden overheating and RF breakdown

- MP conditioning with **NO** bias
- After conditioning, vent with dry nitrogen
- TW max power = 4x SW power to simulate max E/H-field everywhere along the coupler

[27] Z. Zheng, 'Design And Commissioning Of Frib Multipacting Free Fundamental Power Coupler," Proc LINAC2016, p. 767 (2016).

# Coupler High-Power Test Setup: Other Example

**KEK FPC Test and Conditioning Setup (E. Kako [28])**

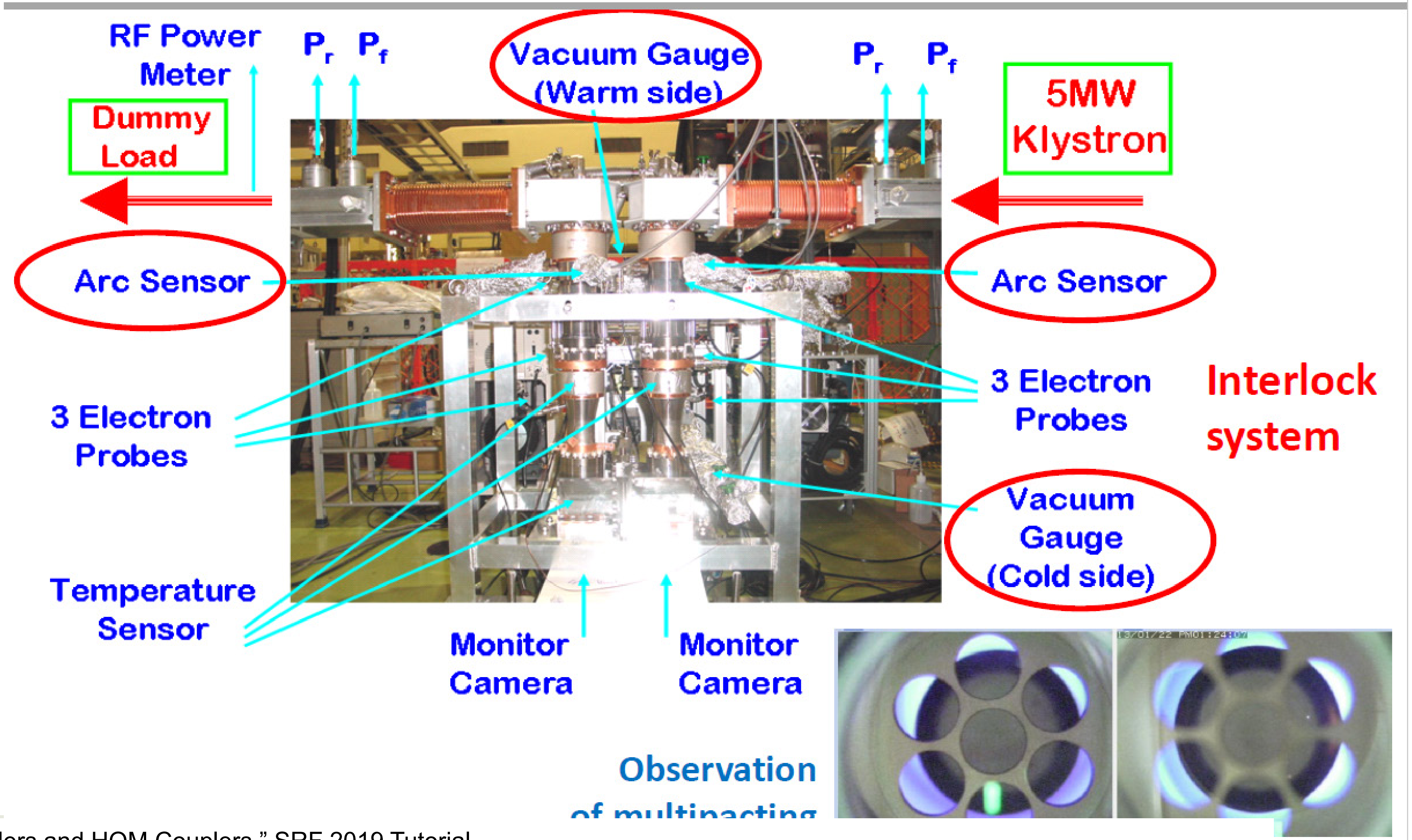


[28] E. Kako, "High Power Couplers and HOM Couplers," SRF 2019 Tutorial.

# Coupler High-Power Test Setup: Other Example

**Other option:**
**Transmission line setup**
**APS-U HHC Coupler**

**Fiber optic thermometry** allows to measure coaxial inner conductor temperatures:
Claimed to be transparent for RF,
No issues when used with
1.3 GHz CW ~20 kW traveling wave

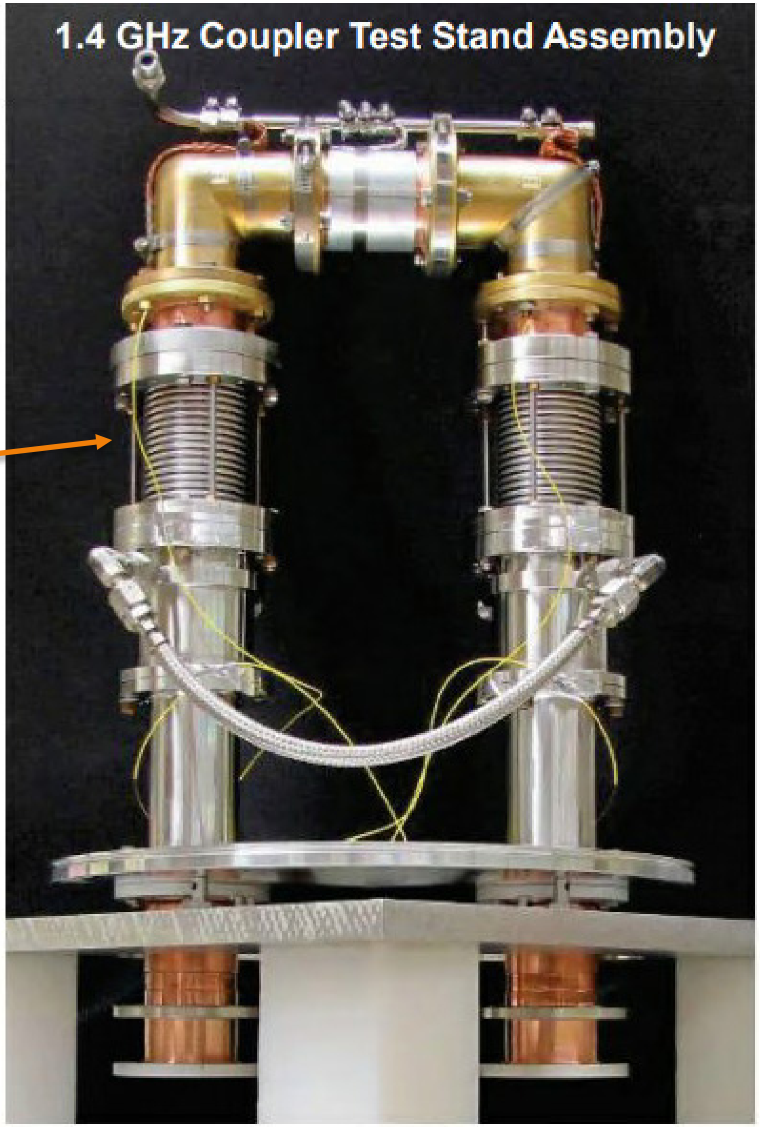


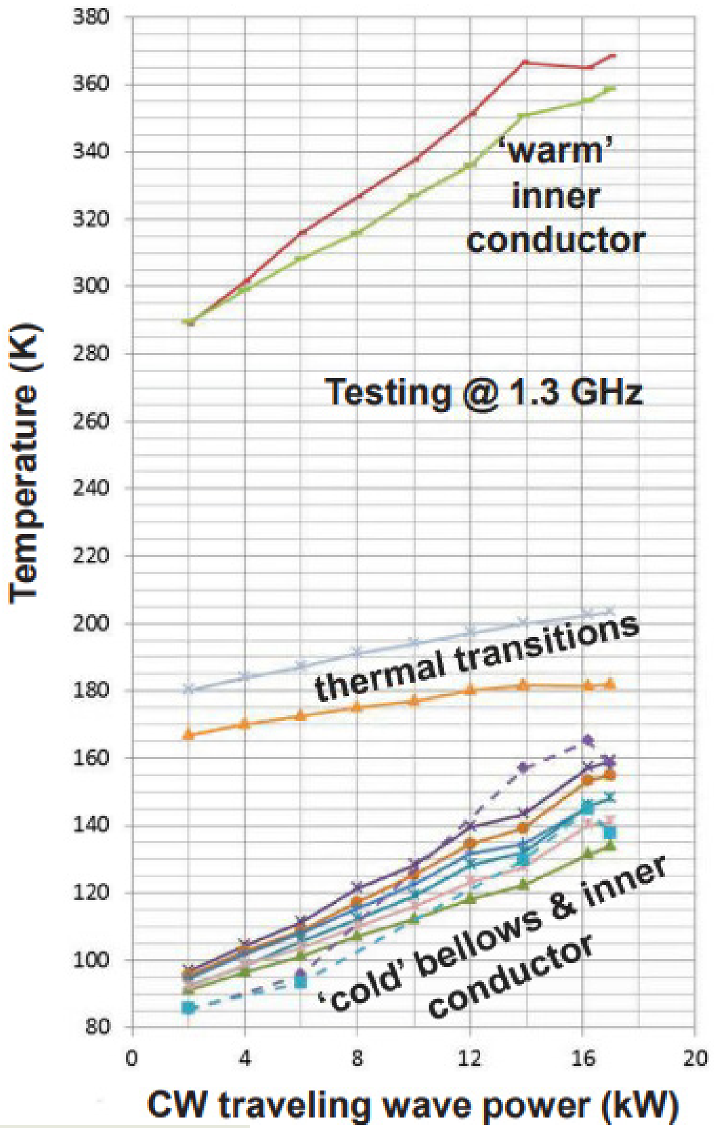

# Test and Operation Integrated with Cavity

- Qext measurements
  - Measure the loaded bandwidth: either frequency sweep (f-domain) or decay time (t-domain)
  - Note that effective Qext could be changed if impedance matching in the transmission line is not good
- Heat load measurements
  - Measure $\Delta T$ and calibrate with a known heater
  - Time constant together with $\Delta T$: can characterize electrical resistivity and thermal conductivity in case of copper plated bellows
- MP
  - Temperature and vacuum response, bias tee dc current is also useful
  - X-rays will appear if MP electrons interact with cavity field
  - Coupler MP should be fully suppressed by conditioning and/or DC bias for reliable cryomodule operation
- Cavity field emission
  - Can enhance coupler MP or cause other (electron-induced) conditioning events
- *Coupler will likely be broken first if your cavity is not good!*

# Concluding Remarks

- High power couplers are one of the most critical components in superconducting cryomodule
  - High power RF along normal conducting walls while minimizing conductive heat leaks
  - Complicated fabrication techniques such as ceramic brazing to metal, copper electroplating, TiN coating
  - Directly exposed to the cavity space so particulate-free as well as grease-free
- Couplers in the existing accelerator facilities with matured operations are based on extensive design, fabrication, and testing efforts
- Nevertheless, you can start from fundamentals, and I hope this helps for you!

# Acknowledgement


- FRIB and ANL colleagues:
  - M. Kelly, S. Kutsaev, T. Xu, S. Miller, P. Ostroumov, A. Plastun
  - In memory of S. Stark, J. Popielarski
- Former SRF tutorial lecturers such as E. Kako and E. Montesinos
- And all the coupler people who brought high power coupler technology to this point

# References


[1] M.P. Kelly, “Coaxial Power Coupler Development at Argonne National Laboratory”, SRF 2017

[2] Y. Kijima et al., “Input coupler of superconducting cavity for KEKB,” Proc. EPAC’00, p. 2040.

[3] E. Montesinos, “Power couplers and HOM dampers at CERN,” ERL17.

[4] I. E. Campisi et al., “the fundamental power coupler prototype for the spallation neutron source (SNS) superconducting cavities,” Proc. PAC2001, p. 1140.

[5] W.D. Moeller, “High power coupler for the TESLA Test Facility,” Proc. SRF1999, p. 577.

[6] V. Veshcherevic et al., “High power tests of first input couplers for Cornell ERL injector cavities,” Proc. PAC07, p. 2355.

[7] S. Belomestnykh and H. Padamsee, “Performance of the CESR superconducting RF system and future plans,” Proc. SRF2001, p. 197.

[8] T. Wangler, “RF Linear Accelerators,” (Wiley-VCH, Weinheim, 2008), pp. 135-148.

[9] T. Wangler, “RF Linear Accelerators,” (Wiley-VCH, Weinheim, 2008), pp. 347-351.

[10] Zinkle, S.J., & Goulding, R.H. (1996). Loss tangent measurements on unirradiated alumina (DOE/ER--0313/19). United States.

# References


[11] N.J. Simon et al., "Properties of copper and copper alloys at cryogenic temperatures," NIST Monograph 117 (1992).

[12] J.E. Jensen, Brookhaven National Laboratory Selected Cryogenic Data Handbook (1980).

[13] R.G. Chambers, "The Anomalous Skin Effect," Proceedings of the Royal Society of London. Series A, Mathematical and Physical Sciences, Vol. 215, No. 1123 (Dec. 22, 1952), pp. 481-497.

[14] W. Signer, D. Dwersteg, "Influence of heat treatment on thin electrodeposited cu layer," Proc SRF'95, p. 653 (1995).

[15] J.G. Hust, A.B. Lankford, "Thermal conductivity of aluminum, copper, iron, and tungsten for temperatures from 1K to the melting point," NBSIR 84-3007 (1984).

[16] NIST Cryogenic Material Properties .

[17] E. Somersalo et al., "COMPUTATIONAL METHODS FOR ANALYZING ELECTRON MULTIPACTING IN RF STRUCTURES," Particle Accelerators, Vol. 59, pp. 107-141.

[18] A.D. Macdonalds, et al., "Microwave Breakdown in Air, Oxygen, and Nitrogen," Phys. Rev. **130**, 1841 (1963).

[19] S. Kim et al., "Design of a 185.7 MHz Superconducting RF Photoinjector Quarter-Wave Resonator for the LCLS-II-HE Low Emittance Injector," Proc. NAPAC2022, p. 245 (2022).

[20] O. Kozlova et al., "Brazing copper to alumina using reactive CuAgTi alloys" Acta Materialia 58 (2010) 1252.

# References

[21] N. Hilleret, “Surface properties of technological materials and their influence on the operation and conditioning of rf coupler,” HPC Workshop (2002).

[22] J.W. Dini, D.D. Snyder, “Electrodeposition of Copper,” Modern Electroplating (2010 John Wiley & Sons, Inc.) pp. 33-77.

[23] https://www.dupont.com/blogs/copper-electroplating-fundamentals.html

[24] H. Kutsuna, T. Ikeda, “Quality control of copper plating for coupler (at Nomura Plating),” LCWS13 (2013).

[25] Y. Okii et al., “R&D of Copper Electroplating Process for Power Couplers: Effect of Microstructures on RRR,” Proc. SRF2019, p. 279 (2019).

[26] T. Xu, “FRIB Cryomodule Design and Production,” Proc. LINAC 2016, p. 673 (2016).

[27] Z. Zheng, ‘Design And Commissioning Of Frib Multipacting Free Fundamental Power Coupler,” Proc LINAC2016, p. 767 (2016).

[28] E. Kako, “High Power Couplers and HOM Couplers,” SRF 2019 Tutorial.